The Vertical Flight Society's 81st Annual Forum & Technology Display
2025. 05. 21 (Wed.)

Vertical Flight Society

Aerodynamic Optimization for Rotor Blade with Structural Design in Hover and Forward Flight

Seongjoong Park[1], Jinwhuy Lee[1], Jeonguk Choi[1], Yu-eop Kang[1], Yoonpyo Hong[2], Gunther Wilke[2], Kwanjung Yee[1]

AVDL Aerospace Vehicle Design Laboratory

DLR Deutsches Zentrum für Luft- und Raumfahrt German Aerospace Center

[1]Seoul National University
Department of aerospace engineering
Aerospace Vehicle Design Laboratory

[2]German Aerospace Center
Institute of Aerodynamics and Flow Technology
Department of Helicopters

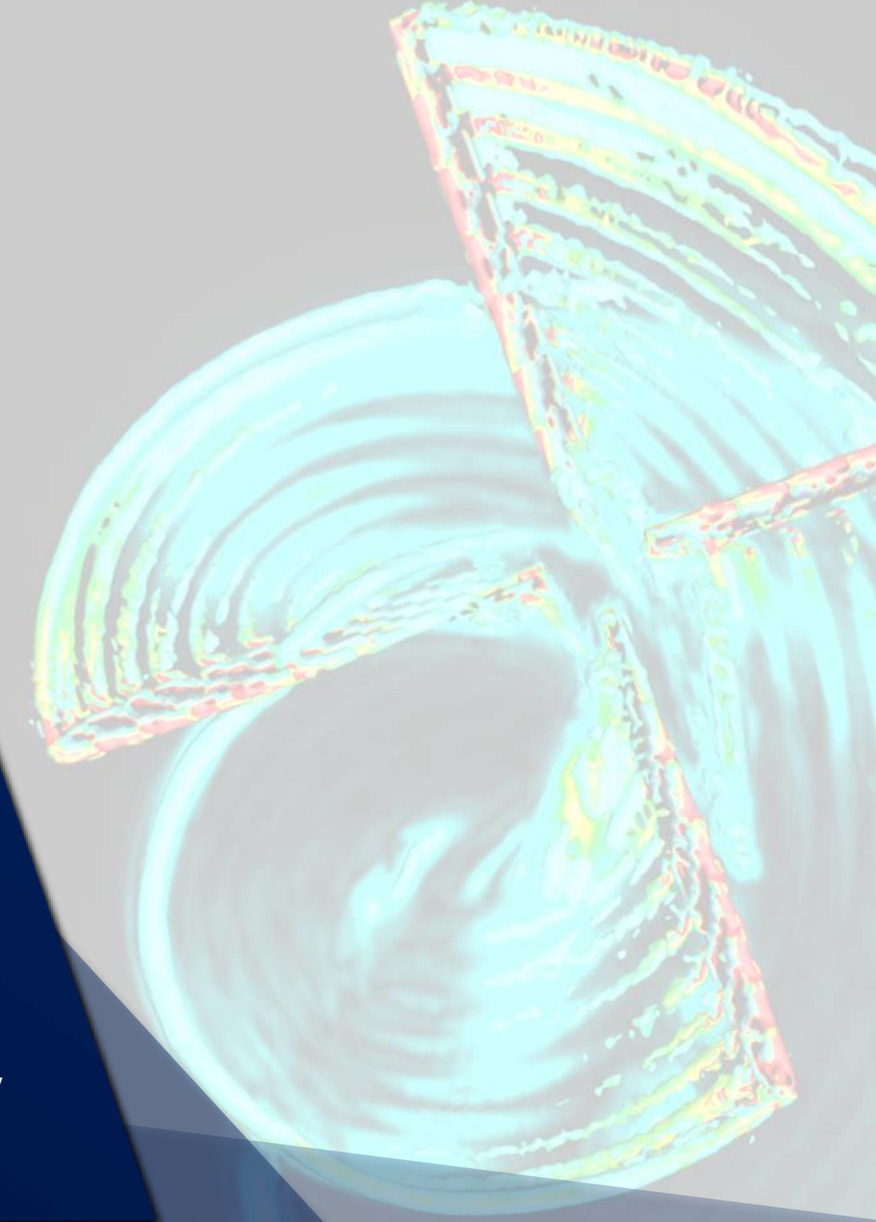

Contents

- Introduction
- Methodology
- Optimization Tasks
- Baseline Results
- Optimization Results
- Conclusion

Contents

- Introduction
- Methodology
- Optimization Tasks
- Baseline Results
- Optimization Results
- Conclusion

INTRODUCTION

[1] Datta, A., *et al.* "Prediction of the UH-60A Main Rotor Structural Loads Using Computational Fluid Dynamics/Comprehensive Analysis Coupling," Journal of the American Helicopter Society, 2008
[2] Celi, R., "Recent Applications of Design Optimization to Rotorcraft-A Survey," Journal of Aircraft, 1999
[3] Smith, M. J., *et al.* "The HART II international workshop: an assessment of the state of the art in CFD/CSD prediction," CEAS Aeronautical Journal, 2013

Research Background

- Rotorcraft offer vertical take-off and landing capability, making them crucial in modern aviation
- However, rotor blades encounter **highly complex aerodynamic environments** during operation[1]
- **Two primary challenges** in blade design:

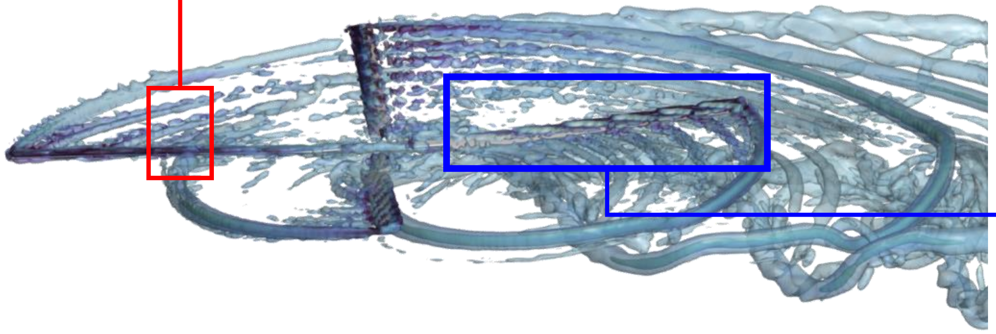

Accounting for complex flow physics[2,3]

- Blade-vortex interaction
- Dynamic stall
- Compressibility effect

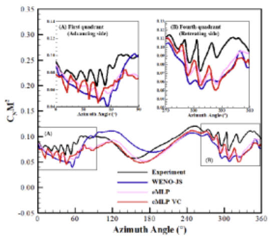

Considering the interaction between aerodynamic and structural characteristics

- Blade aeroelastic behavior
- Blade manufacturability
- Blade resonance

An integrated aero-structural framework is required to reflect multidisciplinary physical interactions during rotor blade optimization

INTRODUCTION

[1] Walsh, J. L., *et al.* "Integrated Aerodynamic/Dynamic/Structural Optimization of Helicopter Rotor Blades Using Multilevel Decomposition," NASA Technical Report NASA TP 3465, 1995
[2] Lim, J., "Consideration of structural constraints in passive rotor blade design for improved performance," The Aeronautical Journal, 2016
[3] Lee, D., *Multi-disciplinary Design Optimization of Rotor Blades using Data-driven Aero-Structure Performance Modeling*, Ph.D. thesis, Seoul National University, 2024
[4] Imiela, M., "High-fidelity optimization framework for helicopter rotors," Aerospace Science and Technology, 2012
[5] Wilke, G., *Aerodynamic Optimization of Helicopter Rotor Blades using Variable Fidelity Methods*, Ph.D. thesis, Technical Univ. of Braunschweig, 2017
[6] Bailly, J., *et al.* "Recent Advances in Rotor Aerodynamic Optimization, Including Structural Data Update," Journal of the American Helicopter Society, 2017

Previous Studies and Limitations

- Prior works performed **sequential aero-structural design**: aerodynamic shape first, structural design later[1,2]
- **Simultaneous design using surrogate models** was also attempted[3]

  → **Low-fidelity solvers were used** in most of these studies, limiting accurate capture of flow physics
- Studies using **high-fidelity CFD often relied on fixed structural assumptions**[4] **or simplified update methods**[5,6] :

  ✓ Scaling methods (e.g., linear scaling, polynomial fitting) to match planform evolution

  → These methods **cannot ensure manufacturing feasibility or satisfaction of dynamic constraints** (e.g., frequency placement, load resistance).

Research Objectives

A high-fidelity simulation-based aero-structural optimization framework is proposed to overcome the limitations

- Validate that the framework produces optimal blades with realistic internal structure that achieve improved FM and L/D.
- Investigate the influence of different structural design and different approaches (actual structural design, scaling method)
- Cross-validate optimization results from different institutions (SNU and DLR) to verify generality

Contents

- Introduction
- **Methodology**
- Optimization Tasks
- Baseline Results
- Optimization Results
- Conclusion

METHODOLOGY

■ *C³* Framework (**C**omprehensive Code + **C**-beam Generator + **C**FD Solver) : Flowchart of the *C³* Framework

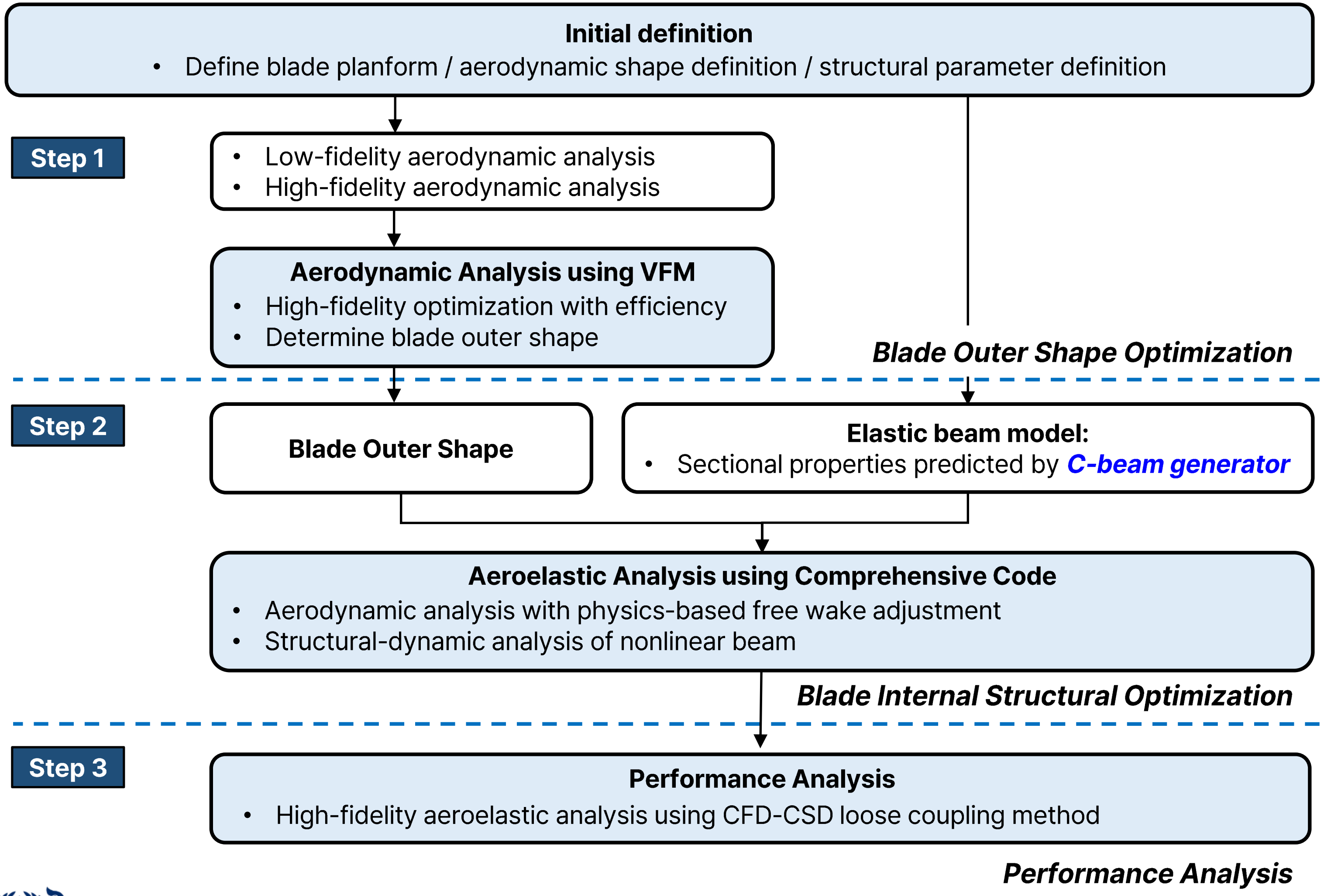

■ Initial definition

- Define design space for blade geometry

■ Step 1: Blade outer shape optimization

- **C**omprehensive Code + **C**FD
- Surrogate based efficient global optimization using variable fidelity modeling(VFM)

■ Step 2: Blade Internal Structural Optimization

- **C**-beam generator + **C**omprehensive code
- Internal structural design satisfying multiple structural dynamic constraints

■ Step 3: Performance Analysis

- **C**omprehensive code + **C**FD
- High-fidelity simulation based aeroelastic performance analysis (CFD-CSD loose coupling)

METHODOLOGY

■ *C³* Framework (**C**omprehensive Code + **C**-beam Generator + **C**FD Solver)

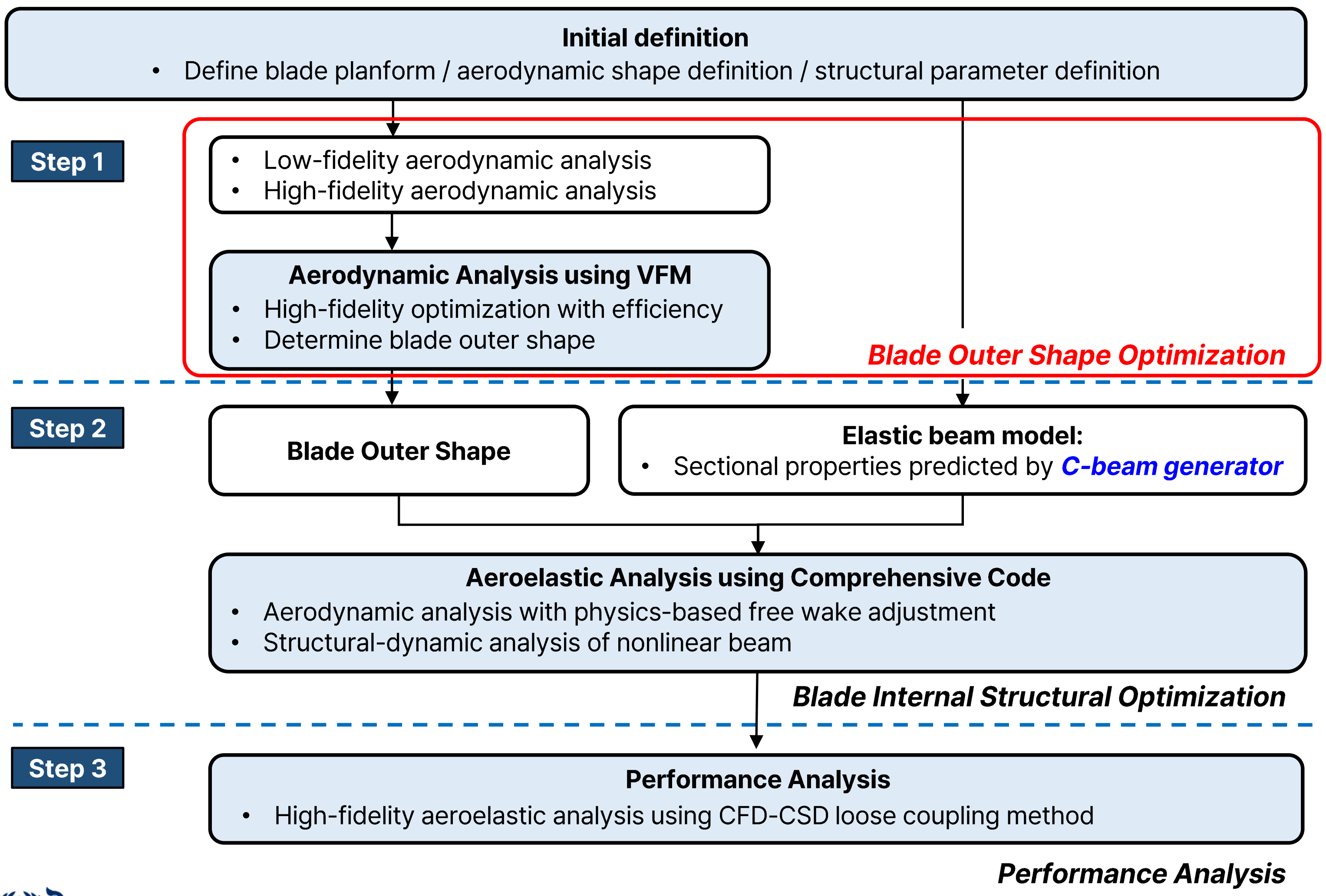

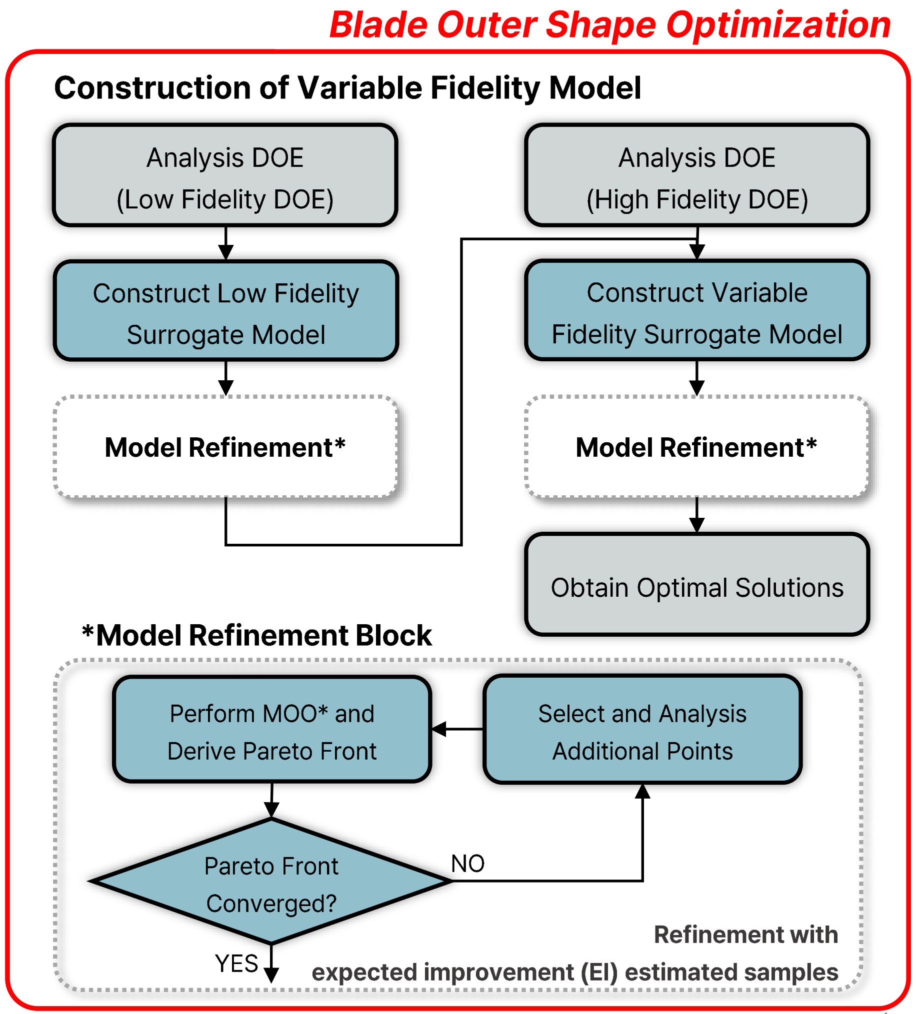

*MOO : Multi-Objective Optimization

METHODOLOGY

[1] Wilke, G., "Variable-Fidelity Methodology for the Aerodynamic Optimization of Helicopter Rotors," AIAA Journal, 2019
[2] Han, Z.-H., *et al.* "Hierarchical Kriging Model for Variable-Fidelity Surrogate Modeling," AIAA Journal, 2012
[3] Johnson, W., "Technology Drivers in the Development of CAMRAD II," American helicopter society aeromechanics specialists conference, 1994
[4] Park, S. H., *et al.* "Implementation of kw turbulence models in an implicit multigrid method," AIAA journal, 2004
[5] Deb, K., *et al.* "An Evolutionary Many-Objective Optimization Algorithm Using Reference-Point-Based Nondominated Sorting Approach, Part I: Solving Problems With Box Constraints," IEEE Transactions on Evolutionary Computation, 2014
[6] Wilke, G., "Quieter and Greener Rotorcraft: Concurrent Aerodynamic and Acoustic Optimization," CEAS Aeronautical Journal, 2021
[7] J. Raddatz *et al.* "Block Structured Navier-Stokes Solver FLOWer," MEGAFLOW - Numerical Flow Simulation for Aircraft Design, 2005
[8] Storn, R *et al.* "Differential Evolution - A simple and efficient adaptive scheme for global optimization over continuous spaces," Journal of Global Optimization, 1997

Blade Outer Shape Optimization

- Surrogate model-based optimization

SNU

Variable Fidelity Modeling (Hierarchical Kriging)[1,2]

- Low Fidelity(LF) Solver : CAMRAD II[3] with inflow model
- High Fidelity(HF) Solver : CFD Solver (KFLOW[4])

Efficient Global Optimization

- Multi-objective optimization → Pareto front
- Optimizer : non-dominated sorting genetic algorithm (NSGA-II)[5]

DLR

Single Fidelity Modeling with efficient CFD setup[6]

- High Fidelity(HF) Solver : CFD Solver (FLOWer[7])

Efficient Global Optimization[1]

- Multi-objective optimization with 50% weighting → One optimum
- Optimizer : Differential Evolutionary optimizer[8] coupled with NSGA-II

Blade Outer Shape Optimization

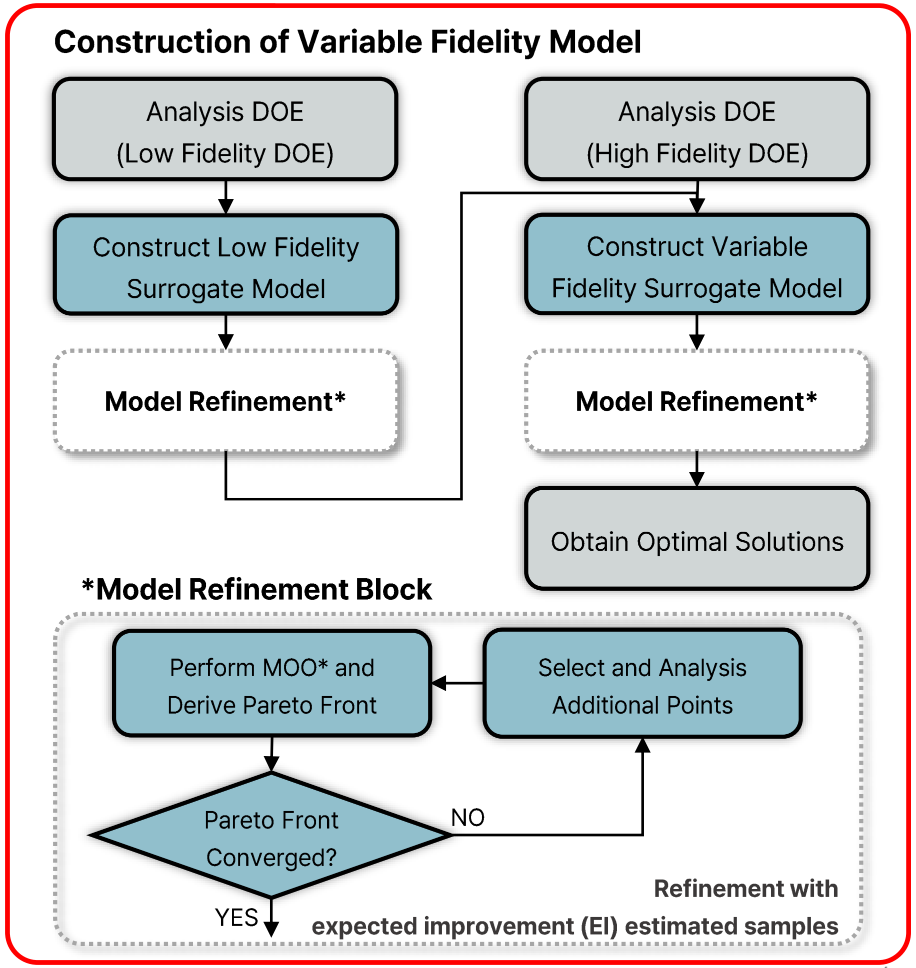

*MOO : Multi-Objective Optimization

Methodology

■ C^3 Framework (Comprehensive Code + C-beam Generator + CFD Solver)

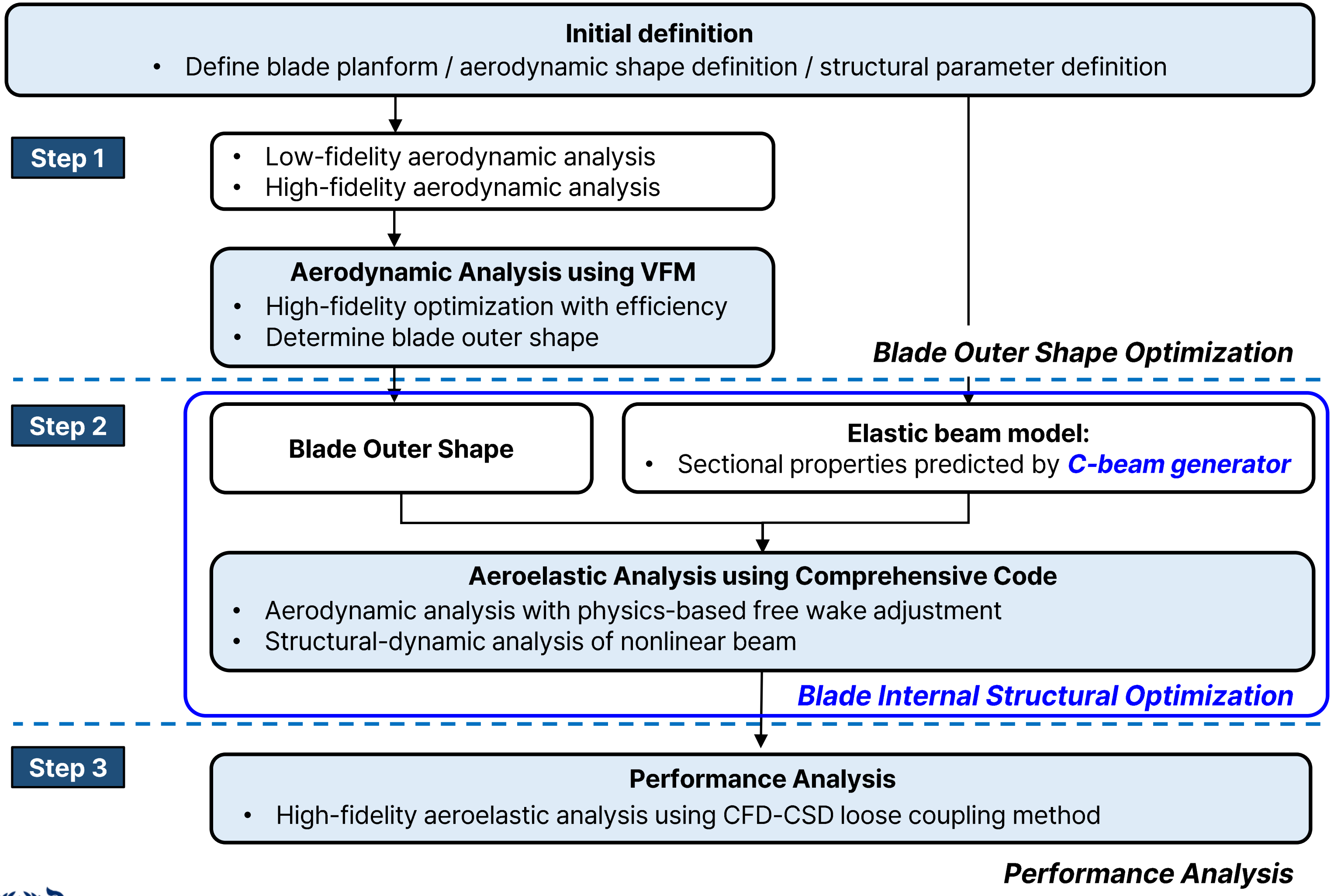

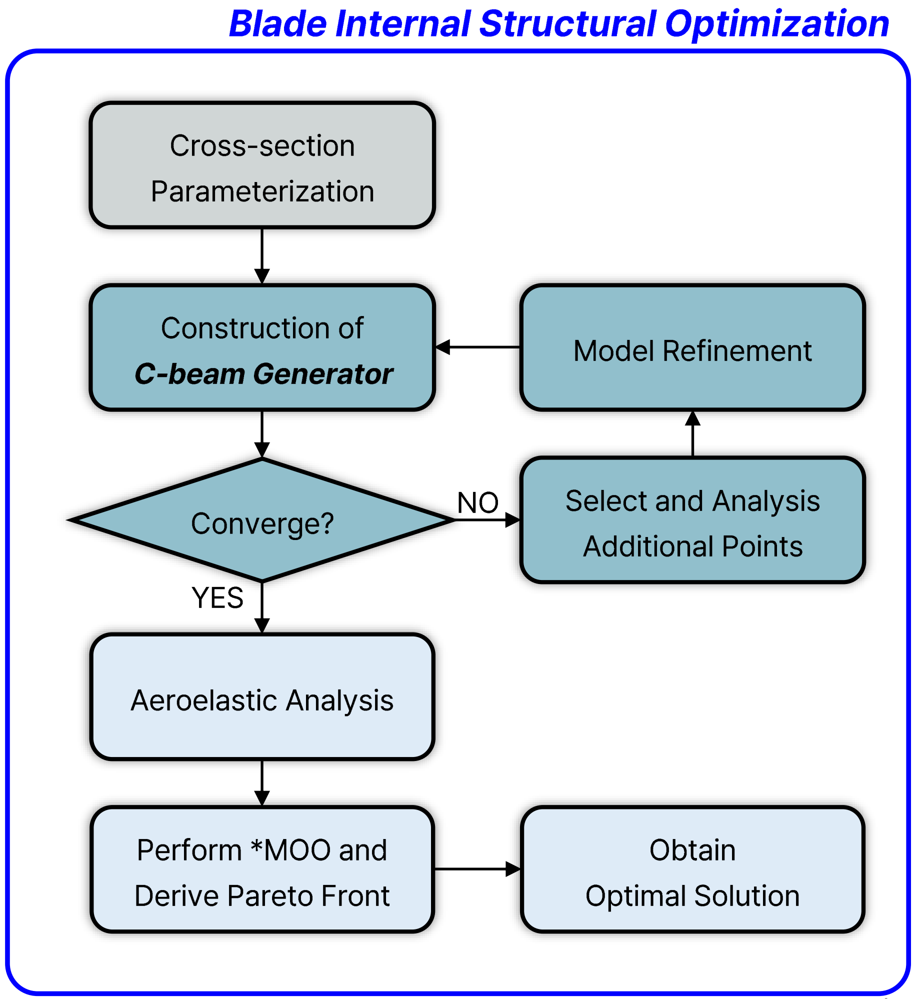

[1] Jung, S., *et al.* "Cross-sectional constants of composite blades using computed tomography technique and finite element analysis," Composite Structures, 2015

METHODOLOGY

Blade Internal Structural Optimization

- Cross-section parameterization
  - ✓ Define design variables based on X-ray scan data[1]

X-ray Scan Data[1] **Parameterization**

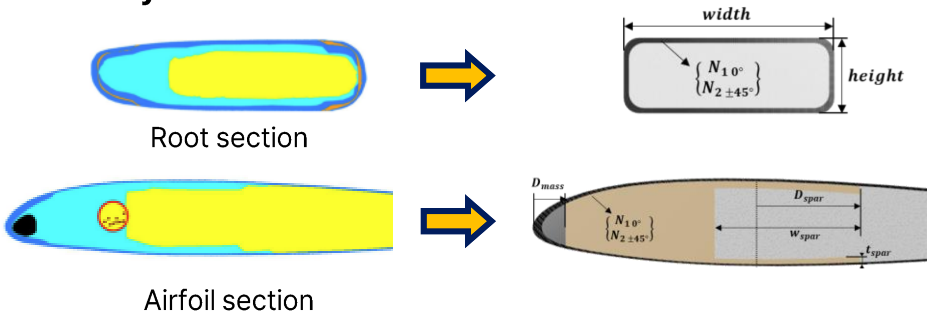

Materials	Glass Epoxy^a	GFRP Block	Lead	Foam
E_{11}, GPa	47.6	23.0	16.0	0.04
E_{22}, GPa	13.3	8.25	16.0	0.04
E_{33}, GPa	13.3	8.25	16.0	0.04
G_{12}, GPa	4.75	3.11	5.6	0.01
G_{13}, GPa	4.75	3.11	5.6	0.01
G_{23}, GPa	4.44	3.11	5.6	0.01
ν_{12}	0.296	0.33	0.28	0
ν_{13}	0.296	0.33	0.28	0
ν_{23}	0.499	0.33	0.28	0
ρ, kg/m^3	1850	1800	11342	60

^{a}Glass Epoxy: S2 Glass Epoxy

▲ Material properties used for cross-section

Design Variables	Root Section (4 DVs)				
	N_1 0°	$N_2 \pm 45°$	height	width	
	Airfoil Section (5 DVs)				
	$N_2 \pm 45°$	t_{spar} [c]	D_{spar}	w_{spar}	D_{mass}

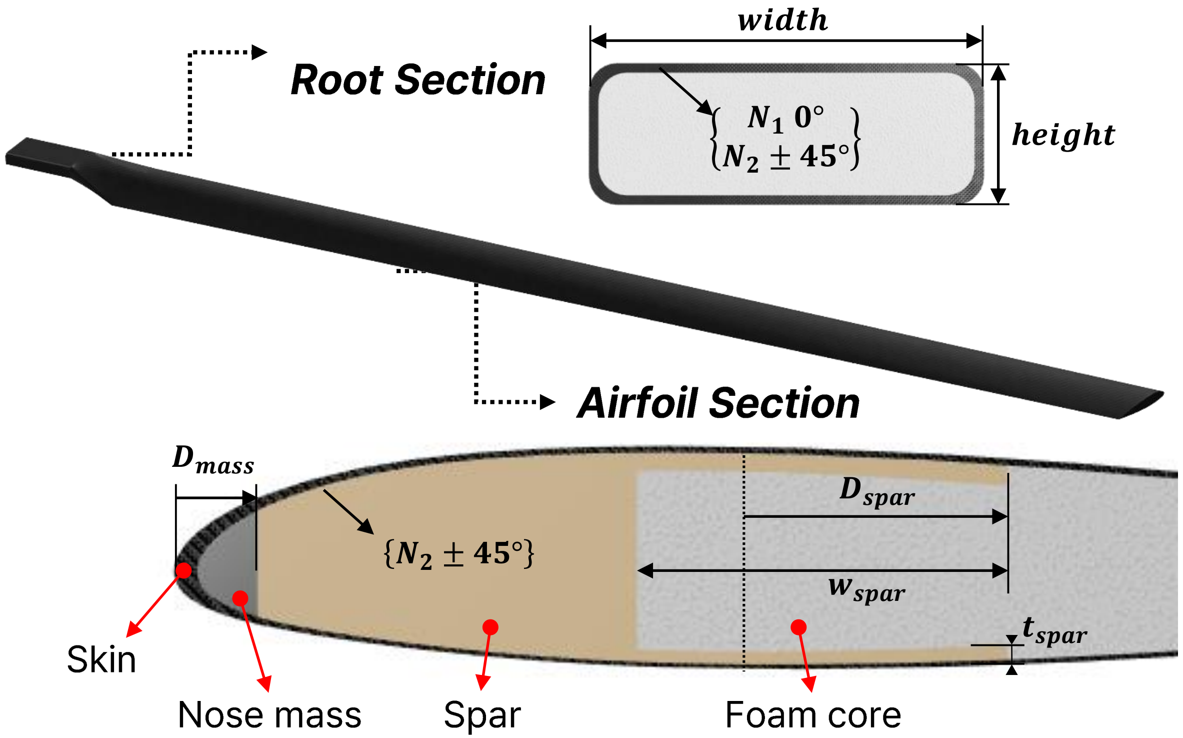

[1] Lee, D., *et al.* "Aeroelastic Design and Comprehensive Analysis of Composite Rotor Blades Through Cluster-Based Kriging," AIAA Journal, Vol. 60, (10), 2022
[2] Jung, S. N., *et al.* "Study on Blade Property Measurement and Its Influence on Air/Structural Loads," AIAA Journal, 2015

METHODOLOGY

Blade Internal Structural Optimization

- Construction of ***C-Beam Generator***[1]
  - ✓ Initial Samples : 100 (Root section), 7500 (Airfoil Section)
  - ✓ Surrogate Model Generation : Gaussian Process Regression
  - ✓ Ksec2d-AE from Konkuk Univ.[2] was used for generating dataset

Cross-Validation results * Predicted Properties (9 Properties) : EA, EIFLAP, EILAG, GJ, MASS, IPOLAR, XI, XEA, XC

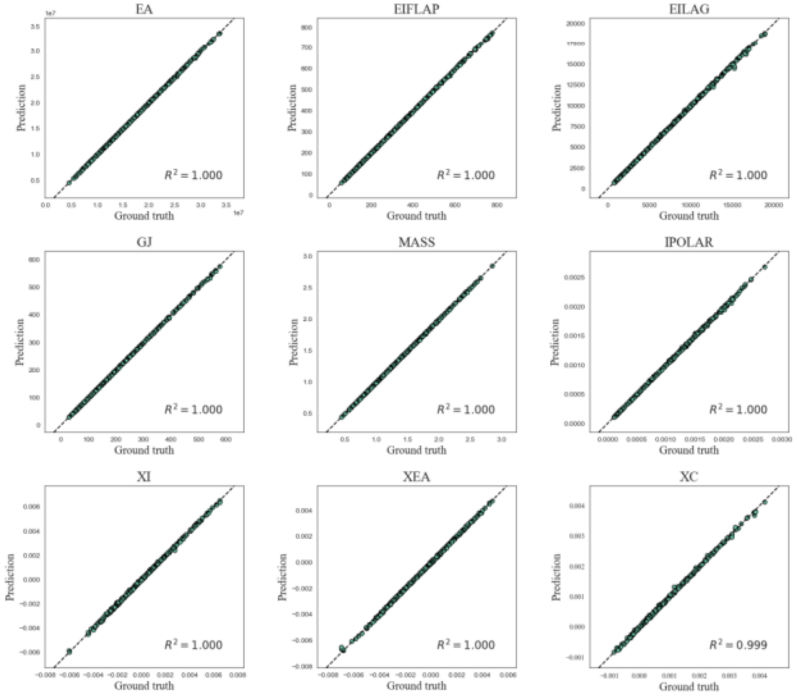

Blade Internal Structural Optimization

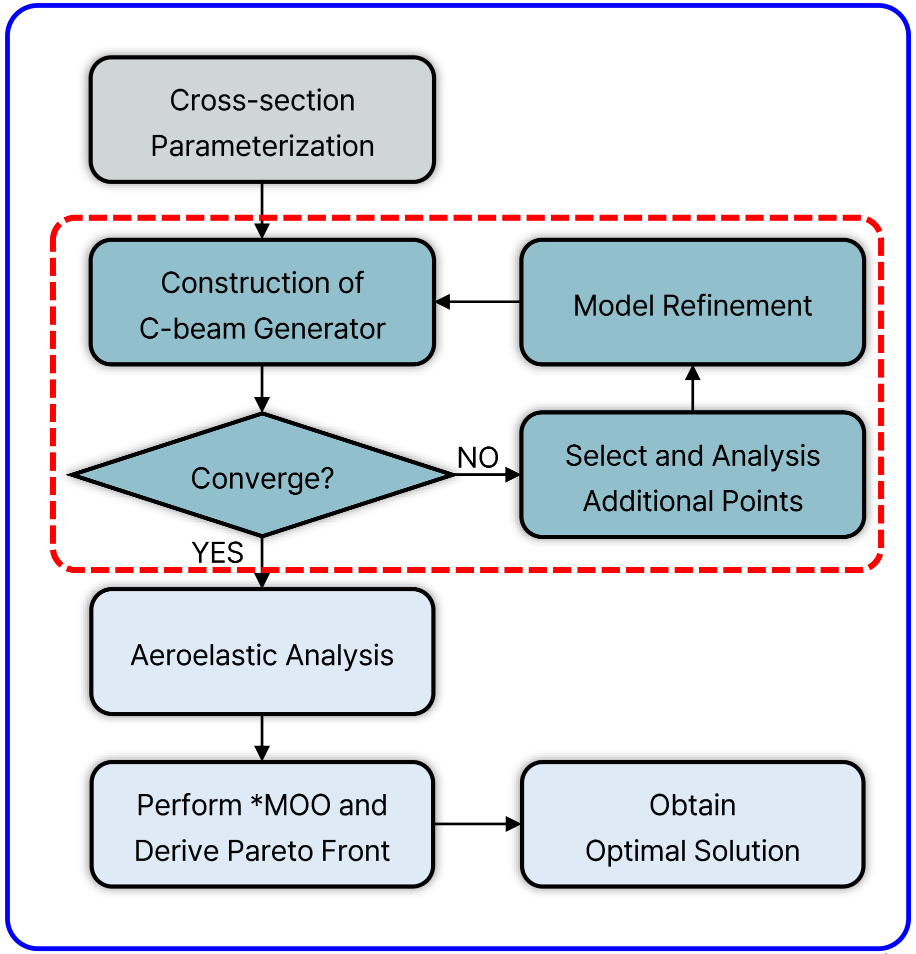

[1] Johnson, W., "Technology Drivers in the Development of CAMRAD II," American helicopter society aeromechanics specialists conference, 1994
[2] Park, S. H., *et al.* "Implementation of kw turbulence models in an implicit multigrid method," AIAA journal, 2004

Blade Internal Structural Optimization

- **Aeroelastic analysis using CAMRAD II** with multiple-trailer wake model[1]

CAMRAD II Aerodynamic model specifications

Reynolds correction	Both lift and drag, $K = \left(\frac{Re}{Re_t}\right)^l, l = 0.2$ Stall Delay Factor with 1.1 (Both lift and drag)
C81 table	from KFLOW URANS solver[2]
Inflow model	General free wake model (Total six multiple-trailer modeled)
Vorticity distribution	Scully Model, $m = 1.0$
Initial tip vortex core radius	$r_c = 0.1\bar{c}$
Core radius growth	Square root, $n = 0.5$
Tip vortex location	0.99R

CAMRAD II Wake Model Validation results

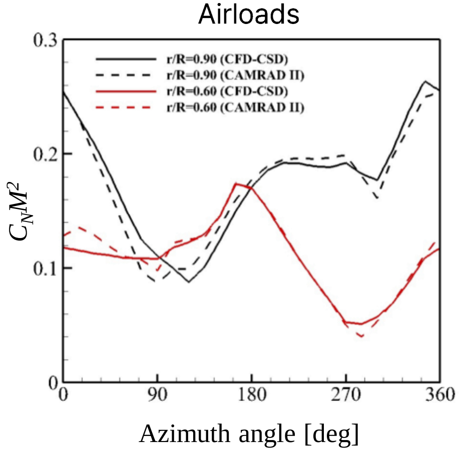

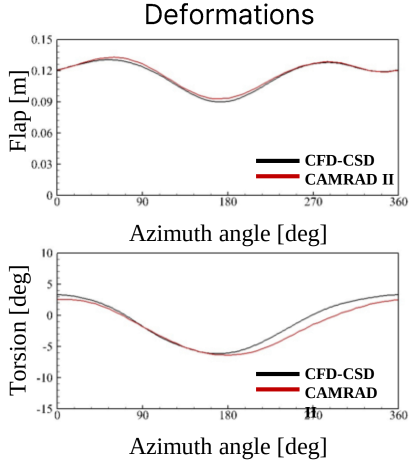

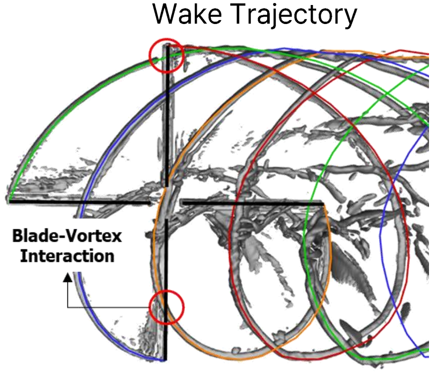

*Overplotted with CFD Q-criterion result
CAMRAD II Wake Trajectory

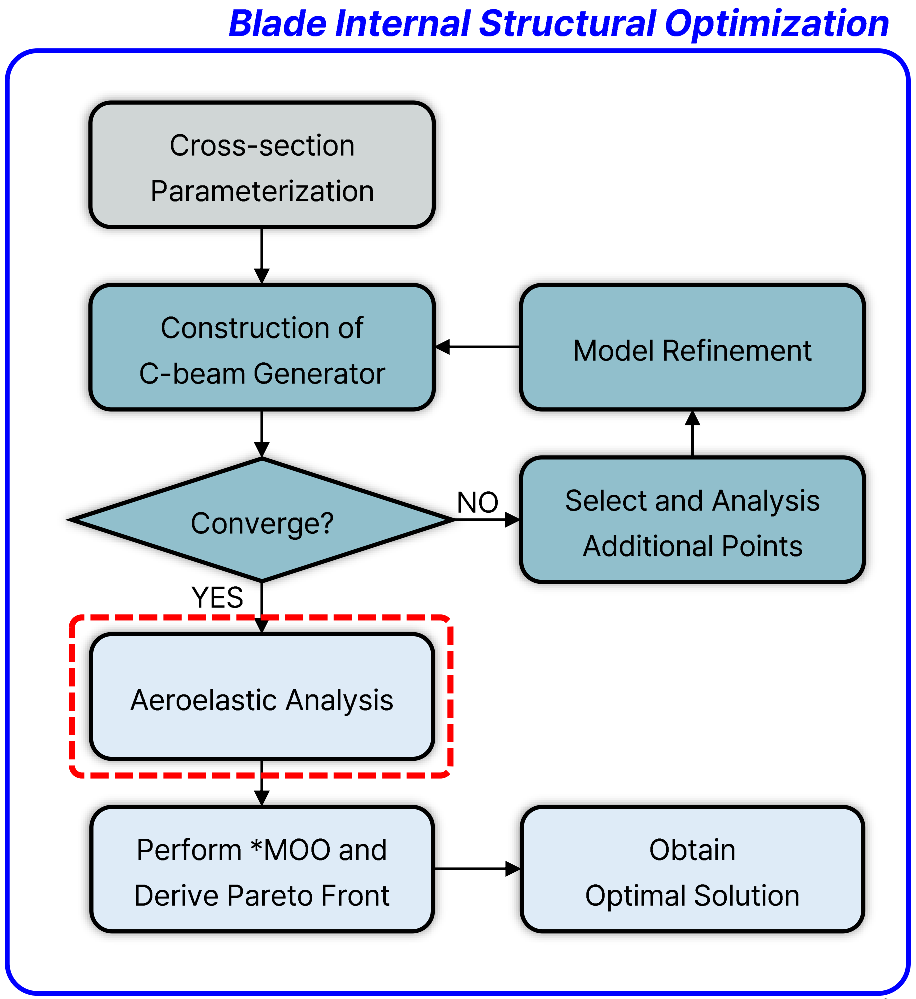

METHODOLOGY

- C^3 Framework (**C**omprehensive Code + **C**-beam Generator + **C**FD Solver)

Initial definition
- Define blade planform / aerodynamic shape definition / structural parameter definition

Step 1
- Low-fidelity aerodynamic analysis
- High-fidelity aerodynamic analysis

Aerodynamic Analysis using VFM
- High-fidelity optimization with efficiency
- Determine blade outer shape

Blade Outer Shape Optimization

Step 2

Blade Outer Shape

Elastic beam model:
- Sectional properties predicted by ***C-beam generator***

Aeroelastic Analysis using Comprehensive Code
- Aerodynamic analysis with physics-based free wake adjustment
- Structural-dynamic analysis of nonlinear beam

Blade Internal Structural Optimization

Step 3

Performance Analysis
- High-fidelity aeroelastic analysis using CFD-CSD loose coupling method

Performance Analysis

Performance Analysis

Final Performance Analysis (CFD-CSD Loose Coupling)

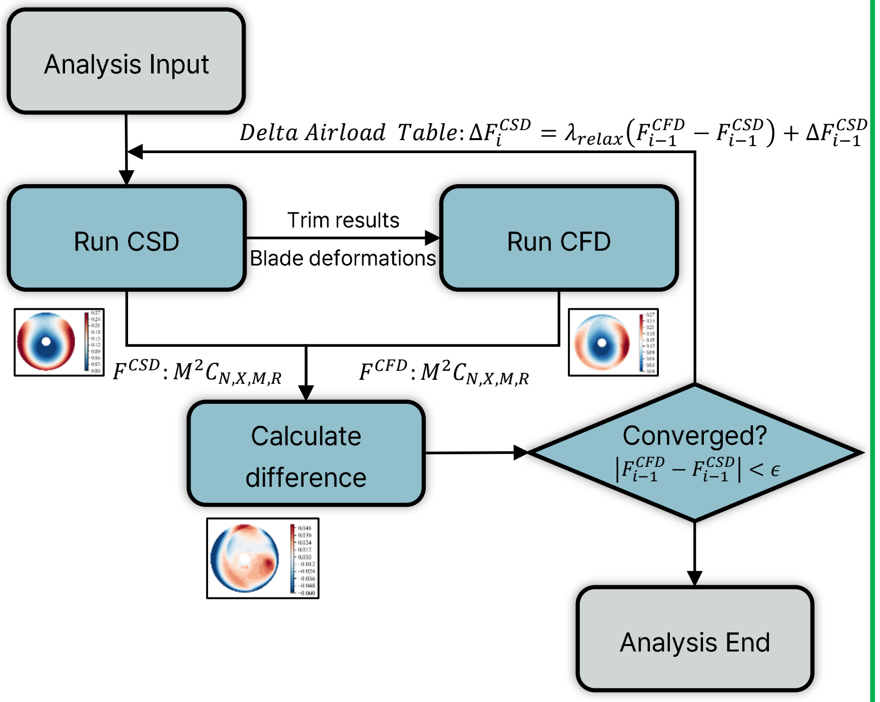

Methodology

Numerical Simulations Setups

[1] Park, S. H., *et al.* "Implementation of kw turbulence models in an implicit multigrid method," AIAA journal, 2004
[2] Hong, Y., *et al.* "Enhanced high-order scheme for high-resolution rotorcraft flowfield analysis," AIAA Journal, 2022
[3] J. Raddatz, and J. K. Fassbender, "Block Structured Navier-Stokes Solver FLOWer," MEGAFLOW - Numerical Flow Simulation for Aircraft Design, edited by N. Kroll and J. K. Fassbender, 2005
[4] K. Kitamura, *et al.* "Towards shock-stable and accurate hypersonic heating computations: A new pressure flux for AUSM-family schemes," Journal of Computational Physics, 2013
[5] V. Vatsa, *et al.* "Re-evaluation of an Optimized Second Order Backward Difference (BDF2OPT) Scheme for Unsteady Flow Applications," 48th AIAA Aerospace Sciences Meeting, 2010
[6] C. C. Heister, "A Method for Approximate Prediction of Laminar-Turbulent Transition on Helicopter Rotors," Journal of the American Helicopter Society, 2018
[7] B. Benoit, A.-M. Dequin, K. Kampa, W. von Grunhagen, P.-M. Basset, and B. Gimonet, "HOST, a ¨ General Helicopter Simulation Tool for Germany and France," 56th Annual Forum of the American Helicopters Society, May 2000
[8] Stanger, C., Hollands, M., Keßler, M., and Kramer, ¨ E., Adaptation of the Dynamic Rotor Blade Modelling in CAMRAD for Fluid-Structure Coupling Within a Blade Design Process, Springer International Publishing, Cham, 2014
[9] Wilke, G., Aerodynamic Optimization of Helicopter Ro-tor Blades using Variable Fidelity Methods, Ph.D. the-sis, Technical Univ. of Braunschweig, 2017

Solver details of CFD Solvers

Solver Details	SNU	DLR
Solver	KFLOW[1]	FLOWer[3]
Inviscid scheme	AUSMPW+ (upwind), 5th order eMLP-VC[2]	SLAU2 scheme (upwind), 4th order van Albada limiter[4]
Temporal Integration	Physical time : BDF2 (Unsteady in cruise), BDF1 (Steady in hover) Pseudo time : DADI	Physical time: BDF2[5] Pseudo time: LU-SGS
Turbulent Model	SA-noft2 (fully turbulent)	SA-DDES-R (with transition model[6])
Rotor motion in (Step1: Outer shape opt.)	**Rigid**	**Elastic** (coupled with HOST[7]) Structure : linear scaling method[8,9])
Rotor motion in (Step3: Performance analysis)	**Elastic** (coupled with CAMRAD II) Structure : designed	**Elastic** (coupled with HOST[7]) Structure : designed
Flight Condition	$C_T/\sigma = 0.1$ in hover, $\mu = 0.3$ in cruise	

Grid Details (Hover)	SNU	DLR
Blade mesh cells	**1.25M**	**2.15M**
Chordwise	170	128
Spanwise	144	128
Normal	50	128
Farfield grids	**15M**	**0.45 M**
Total # of cells	20M	2.6 M
Full rotor equivalent	**20M**	**10.4 M**

Grid Details (Cruise)	SNU	DLR
Blade mesh cells	**1.25M**	**0.25M**
Chordwise	170	80
Spanwise	144	80
Normal	50	40
Farfield grids	**12M**	**3.7 M**
Fuselage	-	0.25M
Total # of cells	**17M**	**4.9 M**

Grid topology

SNU: O-H grid type DLR: O-O grid type

Scaling method[8,9]

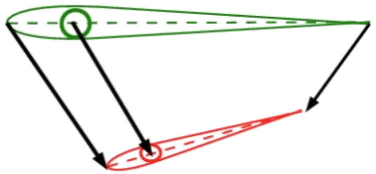

Scaling factor: $\alpha = chord_{new}/chord_{ref}$

Property	Factor
Mass	α
Area	α
Torsional stiffness	α^3
Linear polar inertia	α
Flapping stiffness	α^3
Lead-lag stiffness	α^3

Contents

- Introduction
- Methodology
- **Optimization Tasks**
- Baseline Results
- Optimization Results
- Conclusion

Optimization Tasks

Baseline for Optimization

- **HARTII rotor blade**
  - ✓ Model-scale rotor blade of Bo-105
  - ✓ Features a rectangular planform and hingeless blade design
  - ✓ Widely utilized in various rotorcraft studies due to public availability of structural properties

▲ Bo-105 Helicopter

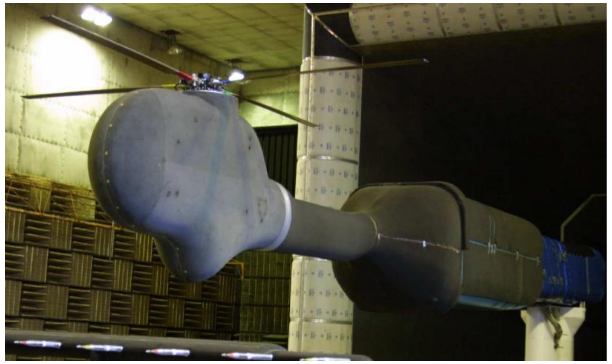

▲ HARTII model

▲ HARTII blade planform

HARTII Rotor Specification	
Rotor type	Hingeless
Shape	Rectangular
Airfoil	NACA23012 with tab
# of Blades	4
Radius	2.0 m
Chord	0.121 m
Twist	-8°/R
Solidity	0.077
Ambient temperature	290.46 K
Ambient pressure	100,970 Pa
RPM	1042
Set thrust	5582 N

▲ HARTII rotor specifications and investigated flight condition

Optimization Tasks

Aerodynamic Design Problem

- Flight condition
  - ✓ Hover : $C_T/\sigma = 0.1$
  - ✓ Cruise : $\mu = 0.3$, $C_T/\sigma = 0.1$, $C_X/\sigma = 0.00944$
- Objective function
  - ✓ Hover : $Maximize\ FM$
  - ✓ Cruise : $Maximize\ L/D_q$
- Design constraint
  - ✓ $\boldsymbol{\sigma}_{thrust-weighted} = const.$
- Design variables (4)
  - ✓ θ/R : Linear twist ratio
  - ✓ $\Delta\theta$: Additional twist added at tip
  - ✓ $chord_1$: Chord length @ r/R=0.75
  - ✓ $chord_2$: Chord length @ r/R=1.00

	Parameter		Lower	Upper
DV1	θ/R	Linear twist ratio	-15	0
DV2	$\Delta\theta$	Additional twist added at tip	-5	5
DV3	$chord_1$	Chord length at r/R = 0.75	1	1.5
DV4	$chord_2$	Chord length at r/R = 1.00	0.5	1.0

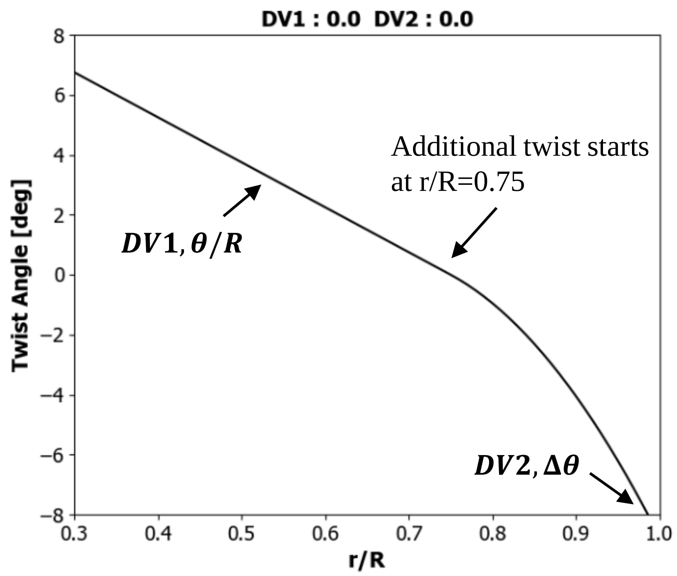

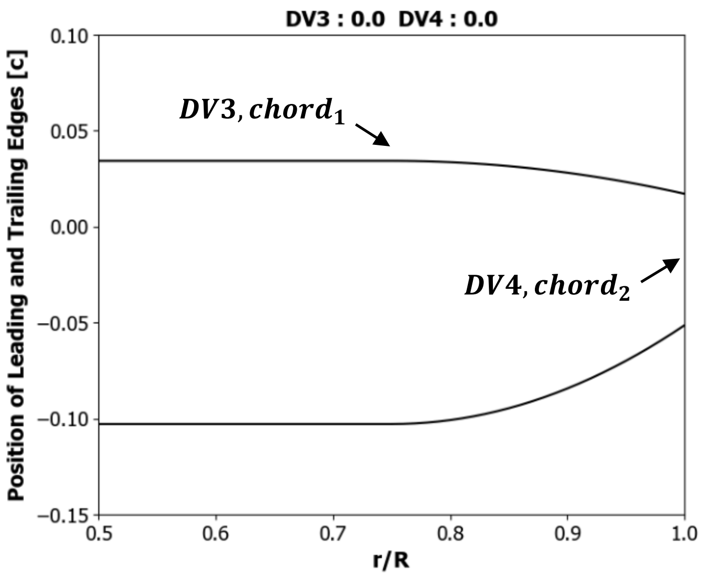

[1] Lee, D., *et al.* "Aeroelastic Design and Comprehensive Analysis of Composite Rotor Blades Through Cluster-Based Kriging," AIAA Journal, Vol. 60, (10), 2022

OPTIMIZATION TASKS

Structural Design Problem

- Objective function
  - ✓ Blade Mass: $Min.\text{Blade Mass}$
  - ✓ Hub Load : $Min.\text{Vibration Index}$ (VI)

$$VI = \sum_{i=NP,2NP} \frac{F_{H,i}}{W_0} + \frac{M_{H,i}}{RW_0} \quad where \quad \begin{cases} F_{H,i} = \sqrt{(0.5F_{xH,i})^2 + (0.67F_{yH,i})^2 + F_{zH,i}^2} \\ M_{H,i} = \sqrt{M_{xH,i}^2 + M_{yH,i}^2} \end{cases}$$

- Constraints
  - ✓ Autorotation Index (AI) : $AI = \frac{I_R\Omega^2}{2W*DL} \geq 0.9 \times AI_{Baseline}$
  - ✓ Tip Flap Deformation : $Tip\ Flap\ Deformation \leq 0.045R$[1]
  - ✓ Dynamic Stability : $0.20c \leq MC. \leq 0.30c\ (CG.: Center\ of\ gravity)$
  - ✓ Frequency placement: 1st Lag, 1st Torsion, 2nd Flap, 2nd Lag, 2nd Torsion, 3rd Flap

$$0.6 \leq g_1(X) = w_{lag}^{1st} \leq 0.8$$
$$2.1 \leq g_2(X) = w_{flap}^{2nd} \leq 2.9$$
$$3.1 \leq g_3(X) = w_{tors}^{1st} \leq 3.9$$
$$4.1 \leq g_4(X) = w_{lag}^{2nd} \leq 4.9$$
$$5.1 \leq g_5(X) = w_{flap}^{3rd} \leq 5.9$$

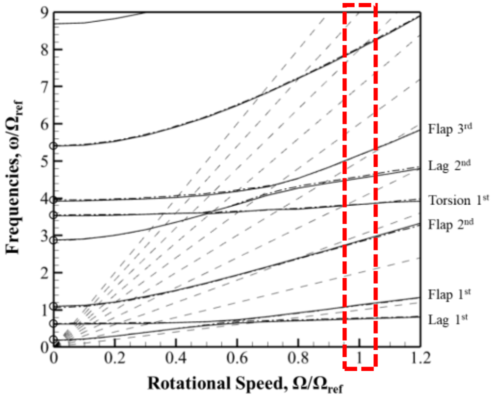

- Design Variables (21 DVs)

1 Root Section

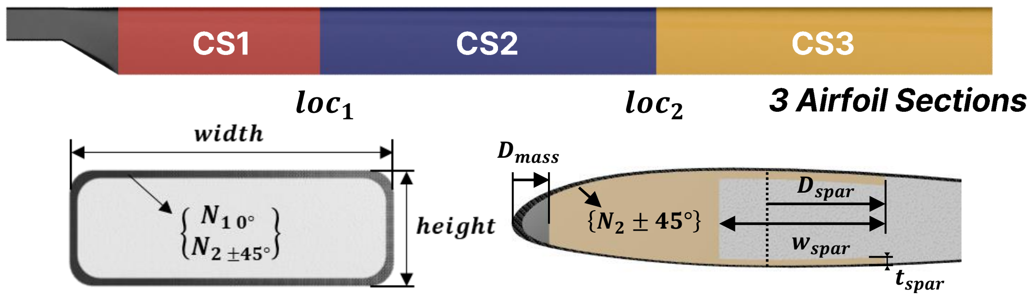

	Design Variables	Lower Bound	Upper Bound
Root Section	$N_1\ 0°$	5	20
	$N_2 \pm 45°$	5	20
	Height [c]	0.13	0.29
	Width [c]	0.37	0.62
Start Location	loc_1	0.3	0.5
	loc_2	0.6	0.8
Airfoil Section (Each)	$N_2 \pm 45°$	2	6
	t_{spar} [c]	0.001	0.015
	D_{spar} [c]	0.1	0.3
	w_{spar} [c]	0	0.2
	D_{mass} [c]	0.05	0.1

Contents

- Introduction
- Methodology
- Optimization Tasks
- **Baseline Results**
- Optimization Results
- Conclusion

BASELINE RESULTS

[1] K¨ufmann, P., *et al.* "The firstwind tunnel test of the DLR's multiple swashplate system: test procedure and preliminary results," 72nd Annual Forum of the American Helicoper Society, 2016

■ Performance Comparison Results for HART II blade from DLR and SNU CFD/CSD solvers

Hover

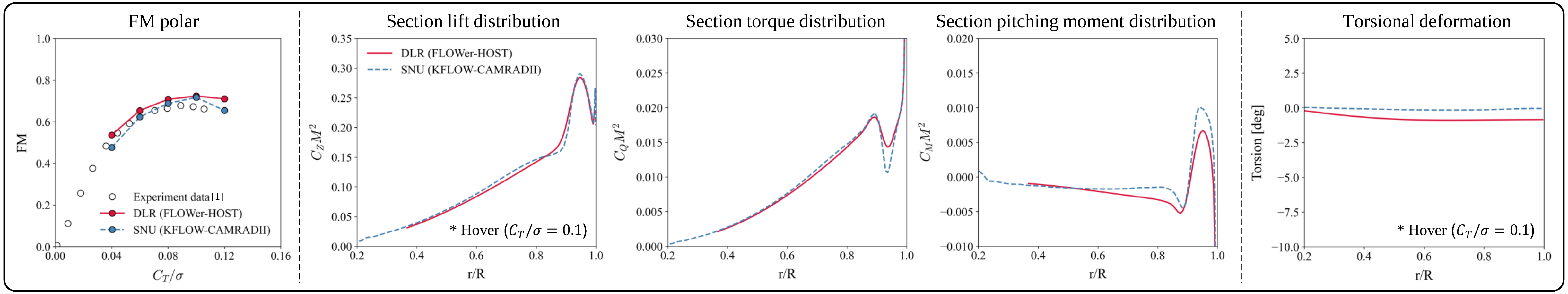

Cruise

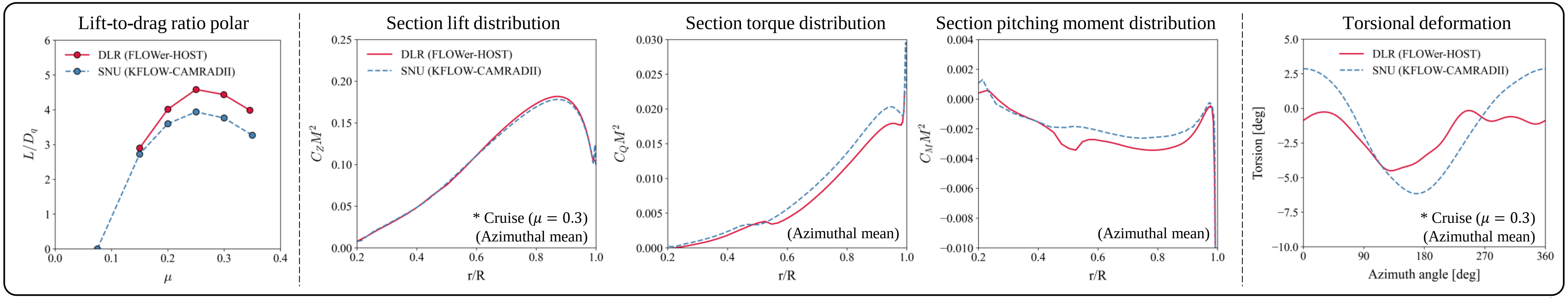

Contents

- Introduction
- Methodology
- Optimization Tasks
- Baseline Results
- **Optimization Results**
- Conclusion

Optimization Results

- **Flight Condition:** $C_T/\sigma = 0.1$, $M_{tip} = 0.64$ (Hover)
  $\mu = 0.3$, $C_T/\sigma = 0.1$, $C_X/\sigma = 0.00944$ (Cruise)

	Parameter		Lower	Upper
DV1	θ/R	Linear twist ratio	-15	0
DV2	$\Delta\theta$	Additional twist added at tip	-5	5
DV3	$chord_1$	Chord length at r/R = 0.75	1	1.5
DV4	$chord_2$	Chord length at r/R = 1.00	0.5	1.0

■ **Step 1:** Aerodynamic Optimization Results (rigid assumed)

- Construction of Variable Fidelity Model(VFM)
  - ✓ Initial 40 Samples from Latin Hypercube Sampling(LHS) method
  - ✓ 6 samples are added for each model update
  - ✓ After 8 iteration, model converged

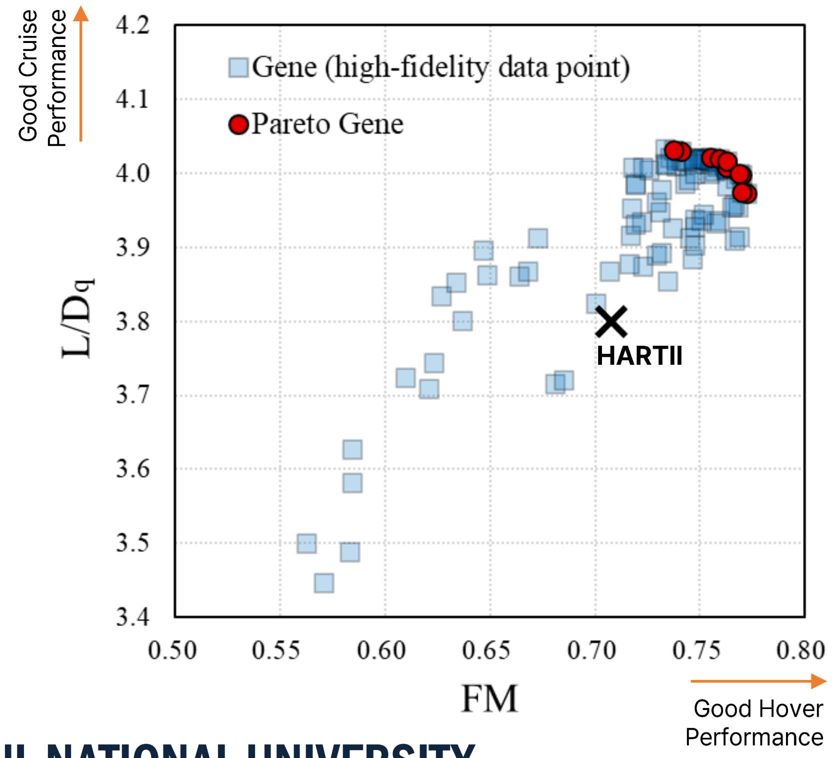

Design contour plots of surrogate models

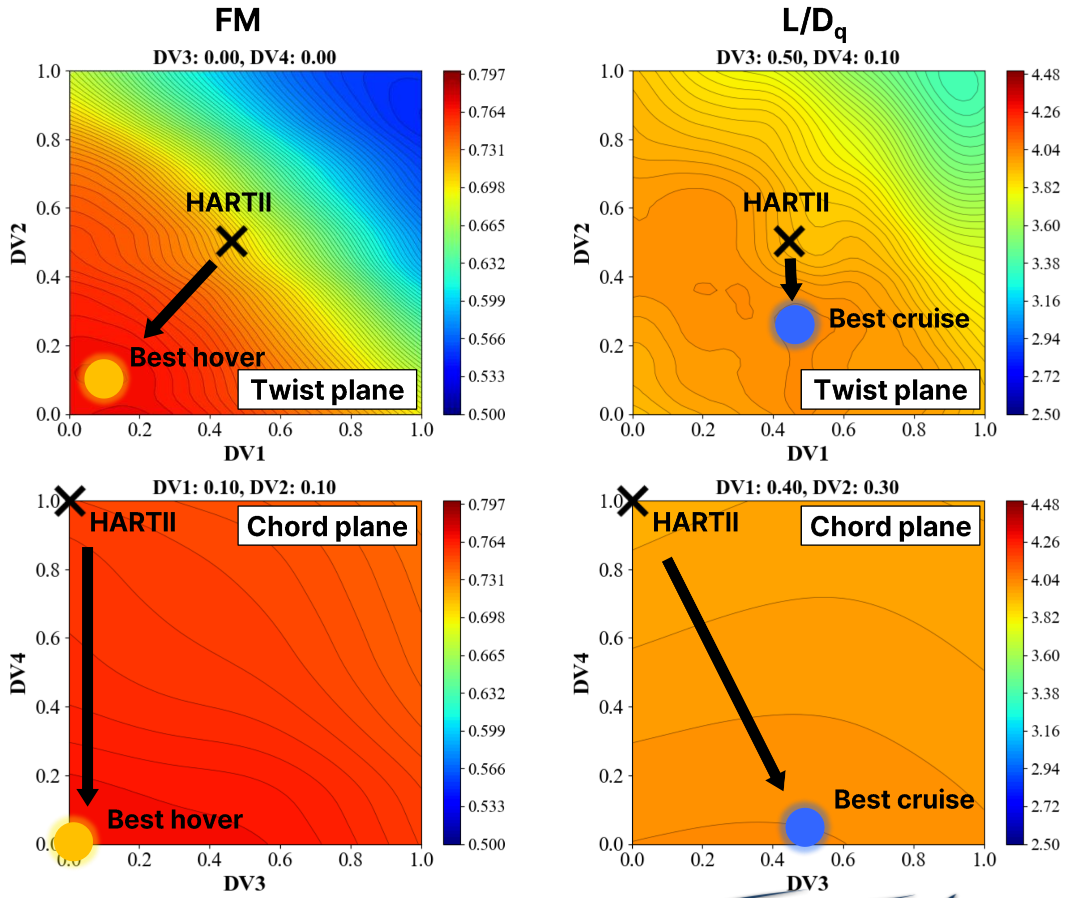

Optimization Results

- **Flight Condition:** $C_T/\sigma = 0.1$, $M_{tip} = 0.64$ (Hover)
  $\mu = 0.3$, $C_T/\sigma = 0.1$, $C_X/\sigma = 0.00944$ (Cruise)

Step 1: Aerodynamic Optimization Results

Optimization results from SNU

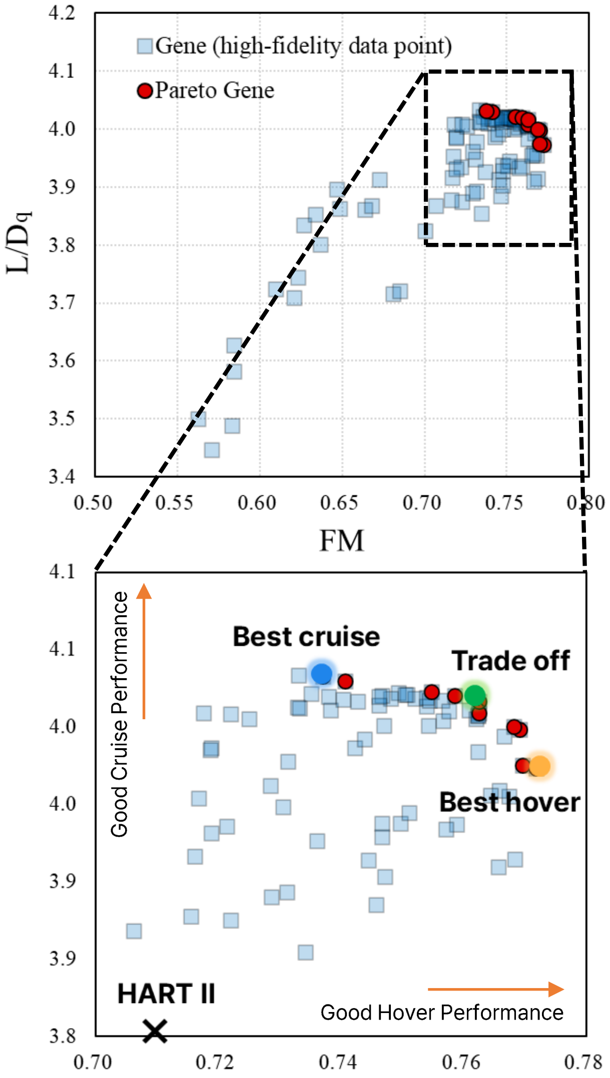

$DV1(\theta/R) = -8°$ $DV2(\Delta\theta_1) = 0.0°$ $DV3(chord_1) = c_{ref}$ * $DV4(chord_2) = c_{ref}$

$DV1(\theta/R) = -5.5°$ $DV2(\Delta\theta_1) = -2.4°$ $DV3(chord_1) = 1.26c_{ref}$ $DV4(chord_2) = 0.57c_{ref}$

$DV1(\theta/R) = -13.2°$ $DV2(\Delta\theta_1) = -4.1°$ $DV3(chord_1) = c_{ref}$ $DV4(chord_2) = 0.5c_{ref}$

$DV1(\theta/R) = -11.6°$ $DV2(\Delta\theta_1) = -2.7°$ $DV3(chord_1) = c_{ref}$ $DV4(chord_2) = 0.5c_{ref}$

$* \ reference\ chord\ length: c_{ref} = 0.121m$

Optimization Results

- **Flight Condition:** $C_T/\sigma = 0.1$, $M_{tip} = 0.64$ (Hover)
  $\mu = 0.3$, $C_T/\sigma = 0.1$, $C_X/\sigma = 0.00944$ (Cruise)

Step 1: Aerodynamic Optimization Results

Optimization results from DLR

Multi-objective optimization with 50% weighting for each object

→ **Single optimal configuration**

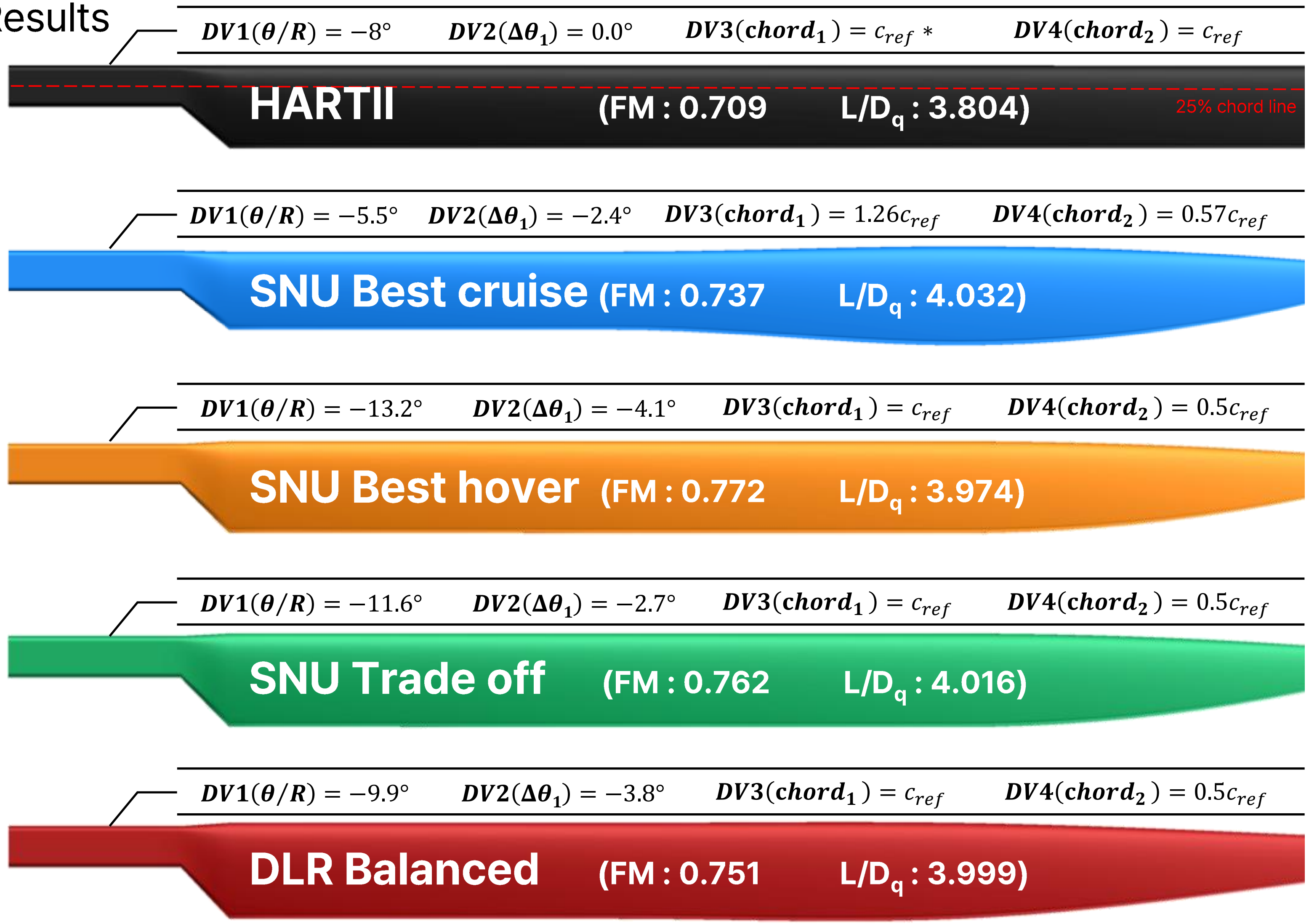

$*$ reference chord length: $c_{ref} = 0.121m$

Optimization Results

- **Flight Condition:** $C_T/\sigma = 0.1$, $M_{tip} = 0.64$ (Hover)
  $\mu = 0.3$, $C_T/\sigma = 0.1$, $C_X/\sigma = 0.00944$ (Cruise)

Step 1: Aerodynamic Optimization Results

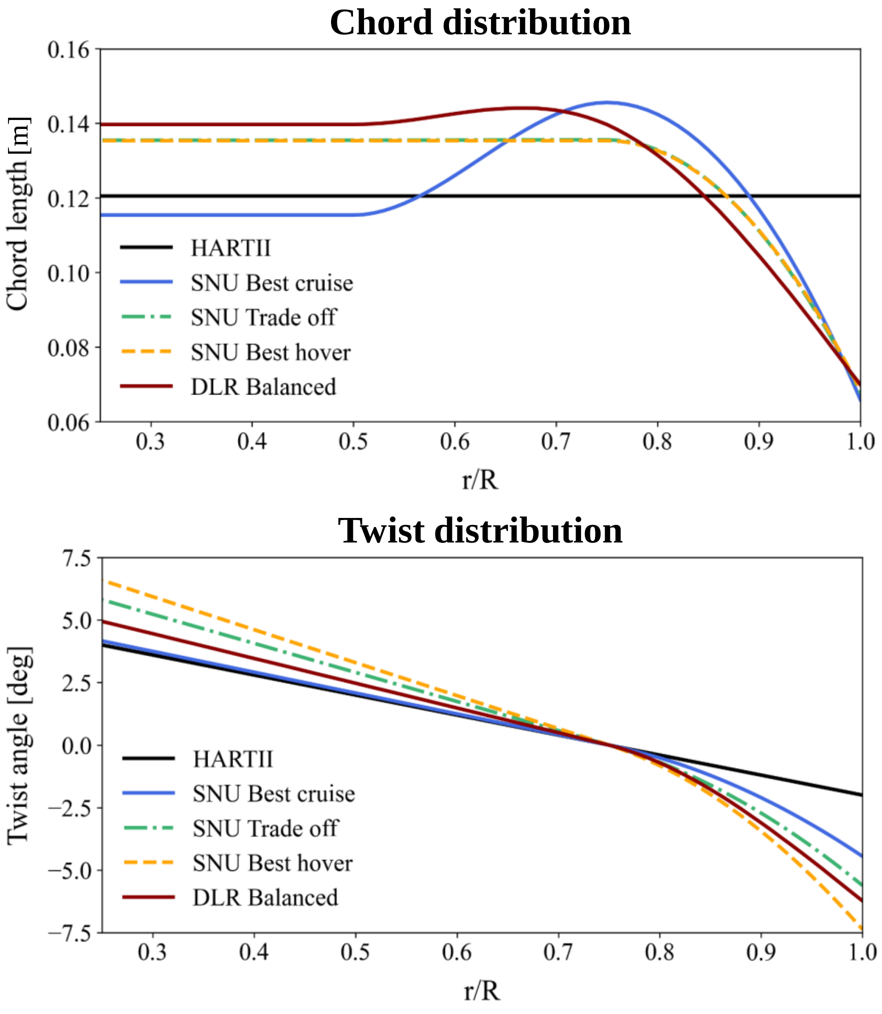

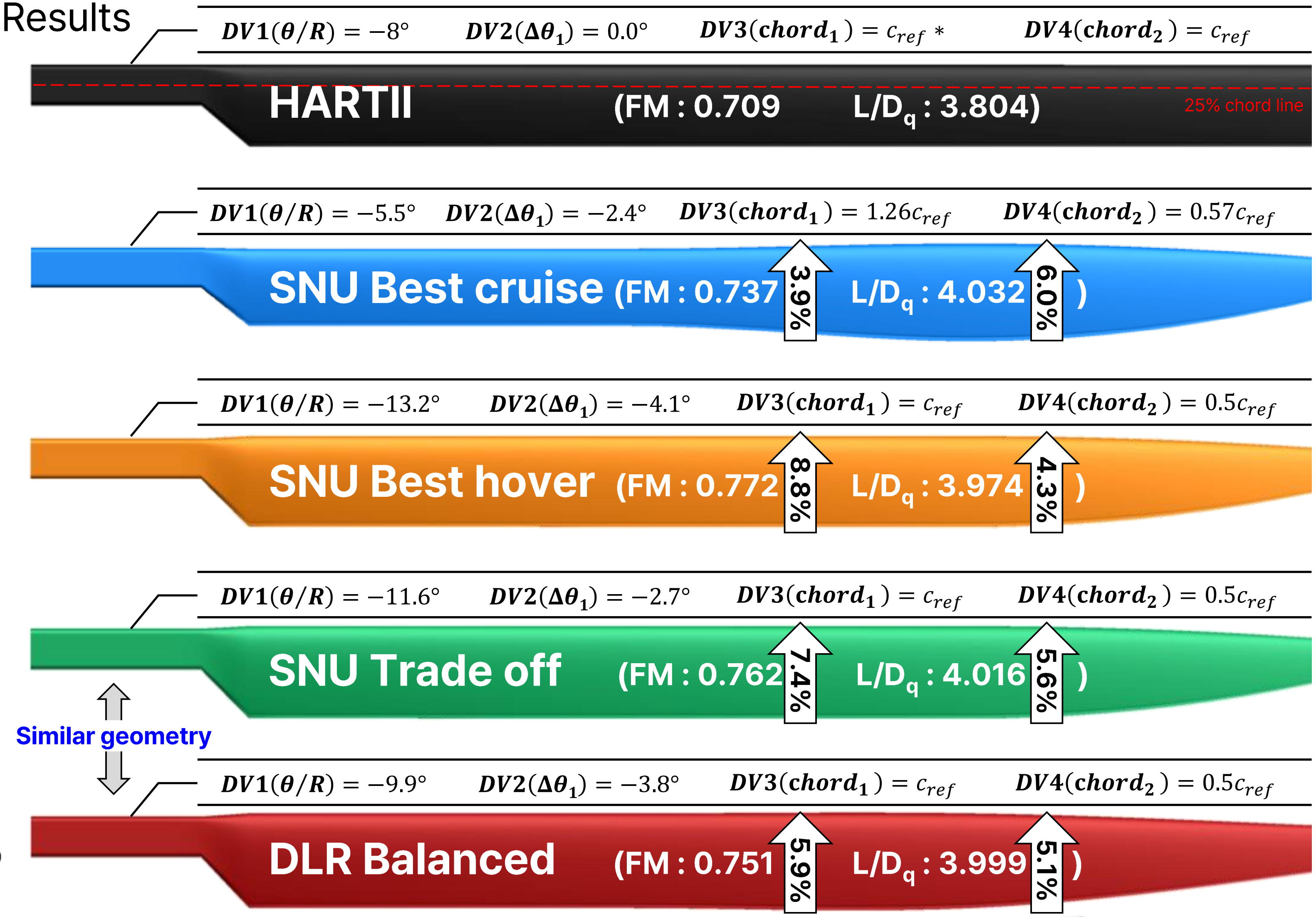

$*$ *reference chord length:* $c_{ref} = 0.121m$

OPTIMIZATION RESULTS

- **Flight Condition:** $C_T/\sigma = 0.1$, $M_{tip} = 0.64$ (Hover)
  $\mu = 0.3$, $C_T/\sigma = 0.1$, $C_X/\sigma = 0.00944$ (Cruise)

Step 2: Structural Optimization Results

- Structural optimizations for (SNU Best cruise / SNU Trade off / SNU Best hover / DLR Balanced) using multi-objective genetic algorithm
  - ✓ **VIs are decreased and masses are increased** (to achieve minimum AI^* and reduce flap deformation at zero precone angle)

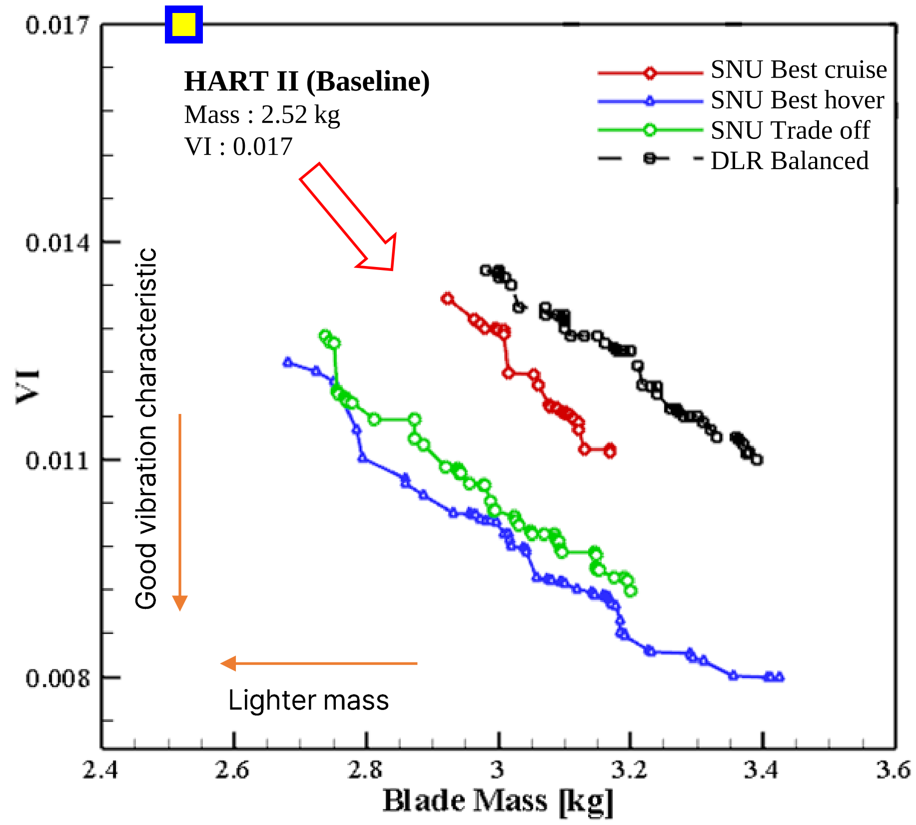

* MV : Minimum Vibration MW : Minimum Weight

$^*AI$: *Autorotation Index*

	HART II (Baseline)	SNU Best hover		SNU Trade off		SNU Best cruise		DLR Balanced	
		MV	MW	MV	MW	MV	MW	MV	MW
Blade Mass	2.52 kg	3.42 kg (35.7%)	2.68 kg (6.3%)	3.20 kg (27.0%)	2.74 kg (8.7%)	3.17 kg (25.8%)	2.92 kg (15.9%)	3.39 kg (34.5%)	2.98 kg (18.3%)
VI	0.0173	0.008 (-53.8%)	0.012 (-28.9%)	0.009 (-46.8%)	0.013 (-26.6%)	0.011 (-35.8%)	0.013 (-23.7%)	0.011 (-36.4%)	0.014 (-21.4%)

Flap deformation at blade tip

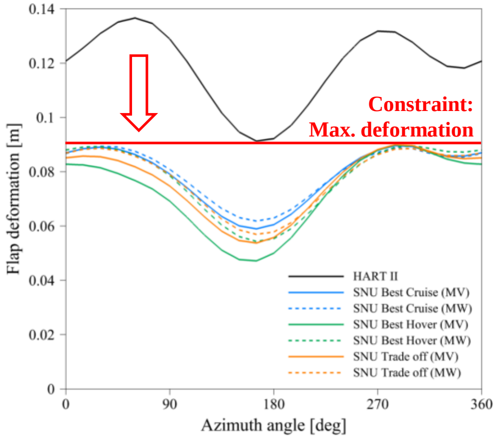

Flap-bending stiffness

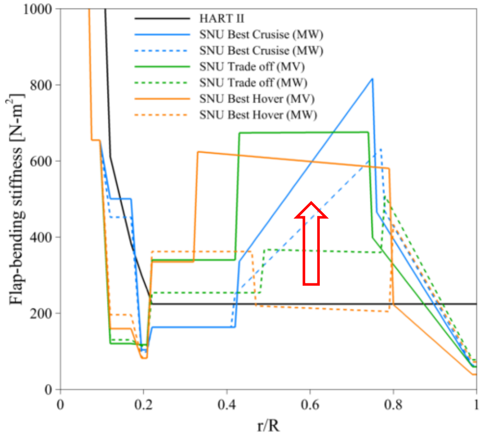

Mass distribution

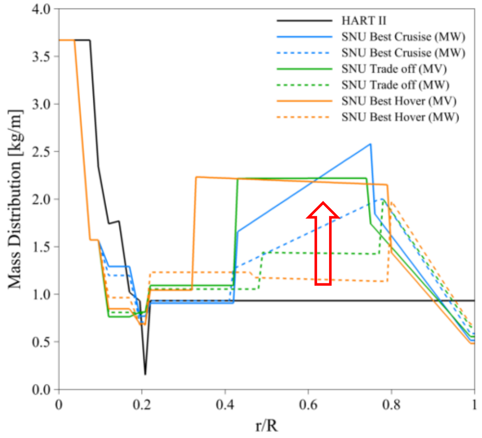

OPTIMIZATION RESULTS

- **Step 3: Final pareto fronts** from **elastic blade** analysis and original pareto front from **rigid blade** analysis
  - Aerodynamic performance comparison
    - ✓ Overall performance outperforms HARTII baseline blade and Pareto trend remains consistent
    - ✓ **Difference between rigid and elastic blade is less than 2%**

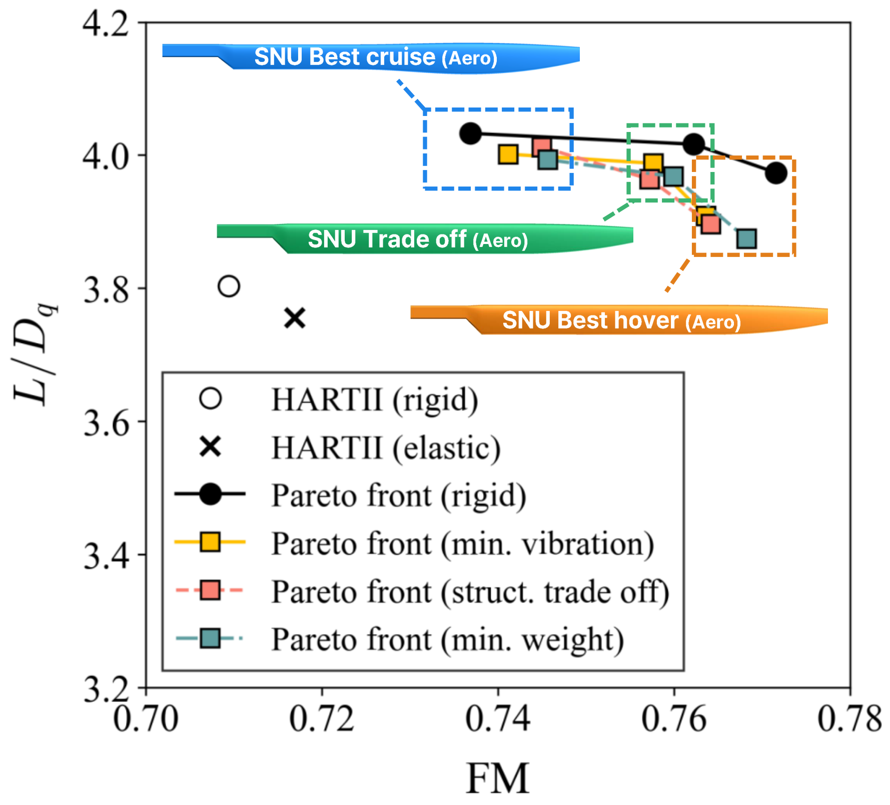

▶ **Hover performance** from **rigid** and **elastic** **blade analysis** using CFD/CSD coupling simulation

	HARTII	SNU Best cruise	SNU Trade off	SNU Best hover
FM_r (rigid)	0.709	0.737	0.762	0.772
FM_e (elastic with min. vibration)	0.717	0.741	0.758	0.764
$\Delta FM = (FM_e - FM_r)/FM_r$	-	**0.6%**	**-0.6%**	**-1.0%**

▶ **Cruise performance** from **rigid and elastic blade analysis** using CFD/CSD coupling simulation

	HARTII	SNU Best cruise	SNU Trade off	SNU Best hover
L/D_{q_r} (rigid)	3.804	4.033	4.016	3.974
L/D_{q_e} (elastic with min. vibration)	3.755	4.001	3.988	3.908
$\Delta L/D_q = (L/D_{q_e} - L/D_{q_r})/L/D_{q_r}$	**-0.8%**	**-0.7%**	**-1.6%**	**-1.0%**

Nomenclature : (r : rigid, e : elastic)

OPTIMIZATION RESULTS

Hover performance analysis (Min. vibration designs)

- Performance gain due to **off-loaded outboard**
  - ✓ Reduced tip AOA due to increased tip twist
  - ✓ Reduced tip chord length

→ Less airload in outboard leads to performance enhancement

Q-criterion colored with vorticity magnitude

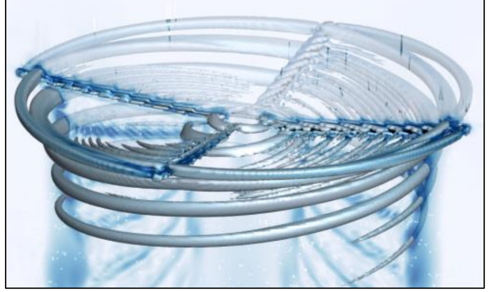

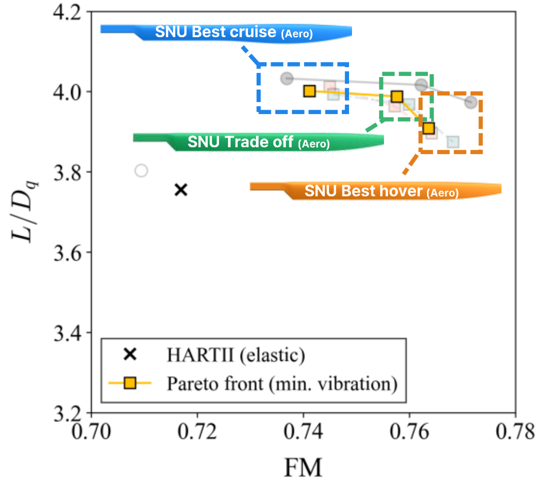

SNU Best hover (FM : 0.764) 6.5%

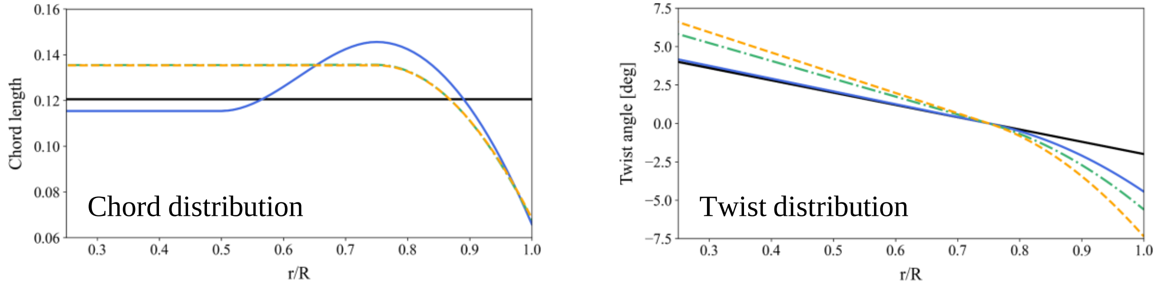

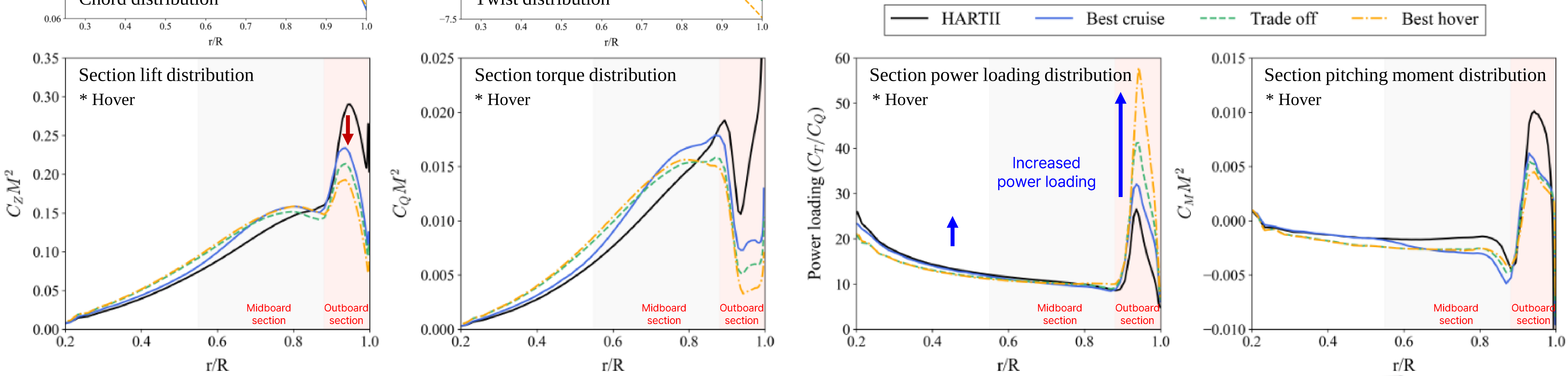

Optimization Results

- **Cruise** performance analysis (Min. vibration designs)
  - **The airload in the tip region is significantly reduced** compared to the HART II blade.
  - **The airload increases** in the midboard section at a radial position of 50%, between azimuth angles of 90° and 180°, which is identified as the **BVI region**

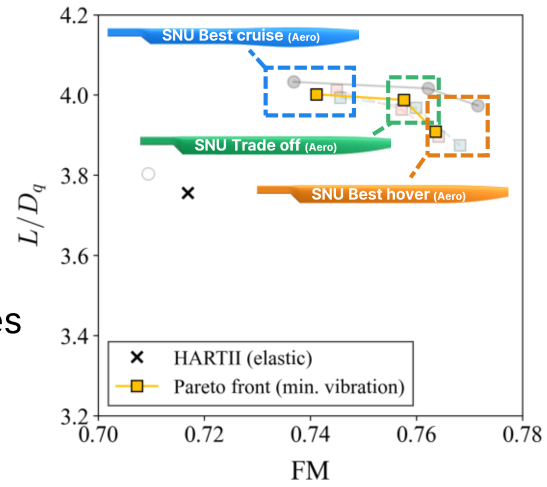

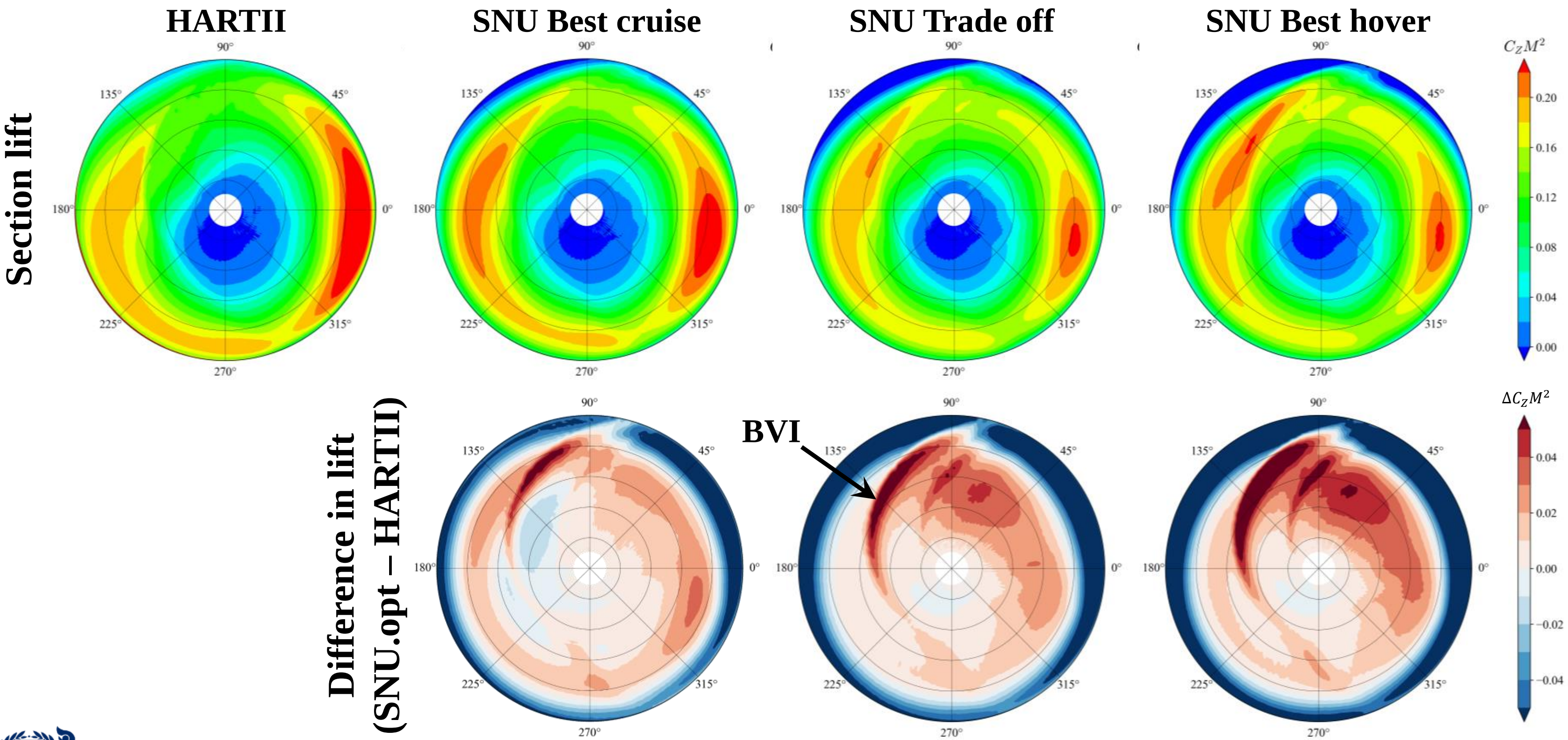

Q-criterion colored with vorticity magnitude

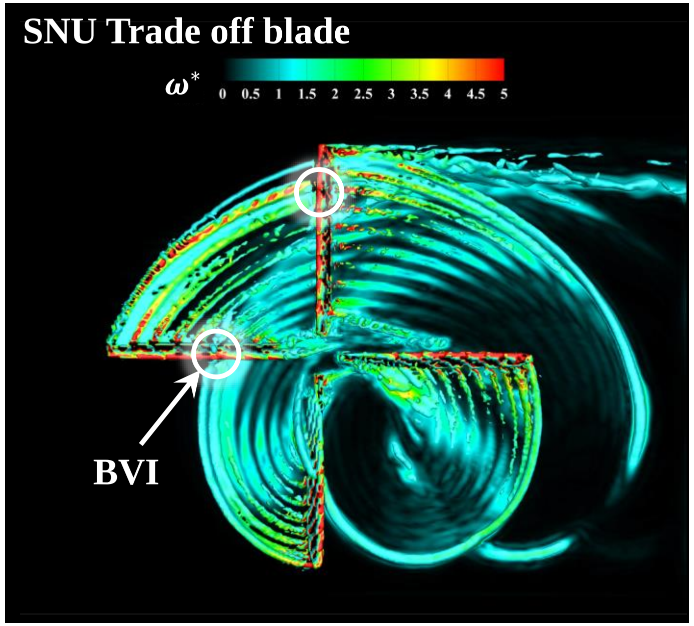

ω^*: non-dimensional vorticity magnitude

OPTIMIZATION RESULTS

- **Cruise** performance analysis (Min. vibration designs)
  - **The torque in the tip region decreases,** while the torque in the midboard region increases
  - The increase in torque in the midboard region of SNU Best cruise blade during the 135° to 270° azimuth range is smaller than other blades → SNU Best cruise blade shows best cruise performance

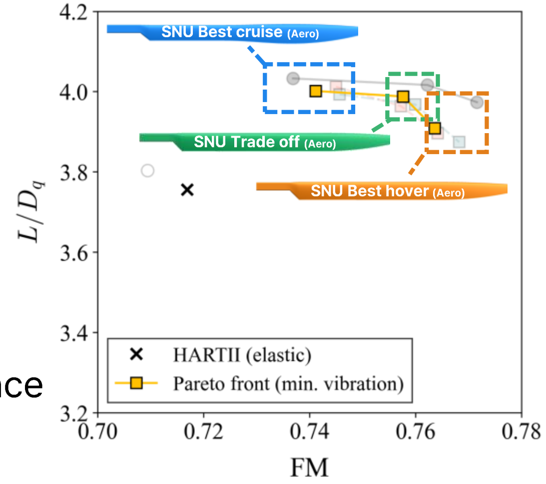

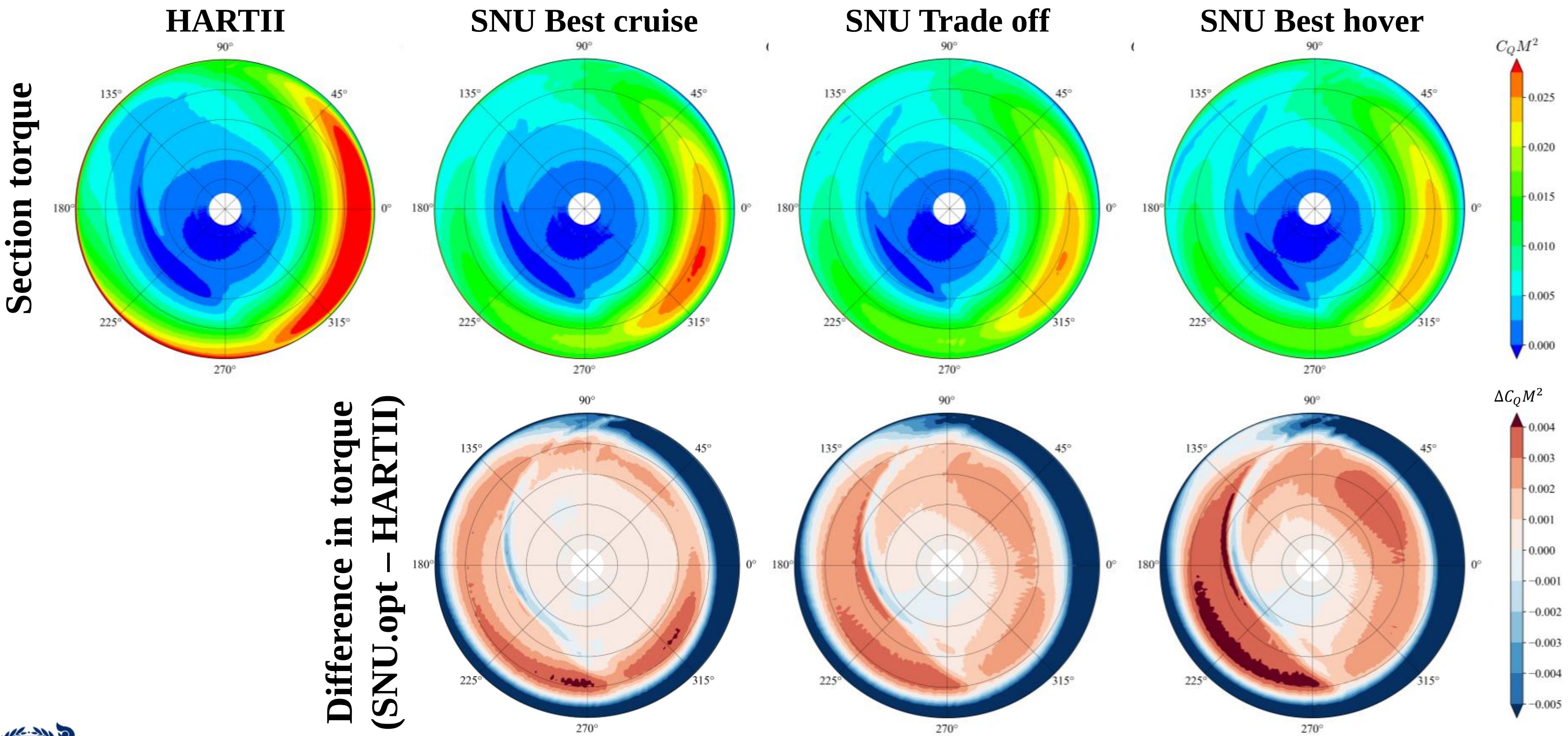

Q-criterion colored with vorticity magnitude

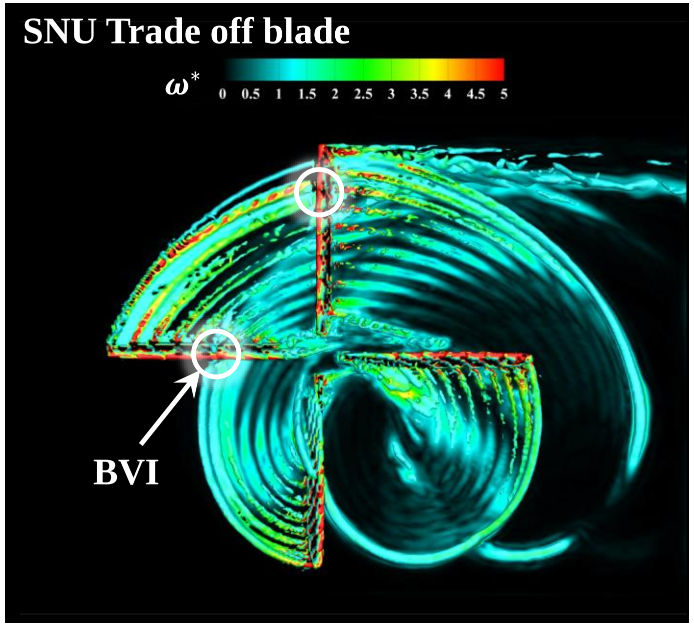

ω^*: non-dimensional vorticity magnitude

Contents

- Introduction
- Methodology
- Optimization Tasks
- Baseline Results
- **Optimization Results : Aeroelastic Implications of Structural Design**
- Conclusion

Aeroelastic Implications of Structural Design

- Aeroelastic Effects of **Different Structural Optimization Objectives** (based on the SNU Trade off blade)
  - Three structure designs (Min. vibration / Struct. Trade off / Min. weight) shows **similar aerodynamic loads**
    - ✓ **Structural design is highly constraint-driven,** requiring satisfaction of numerous constraints → **design space becomes narrow**

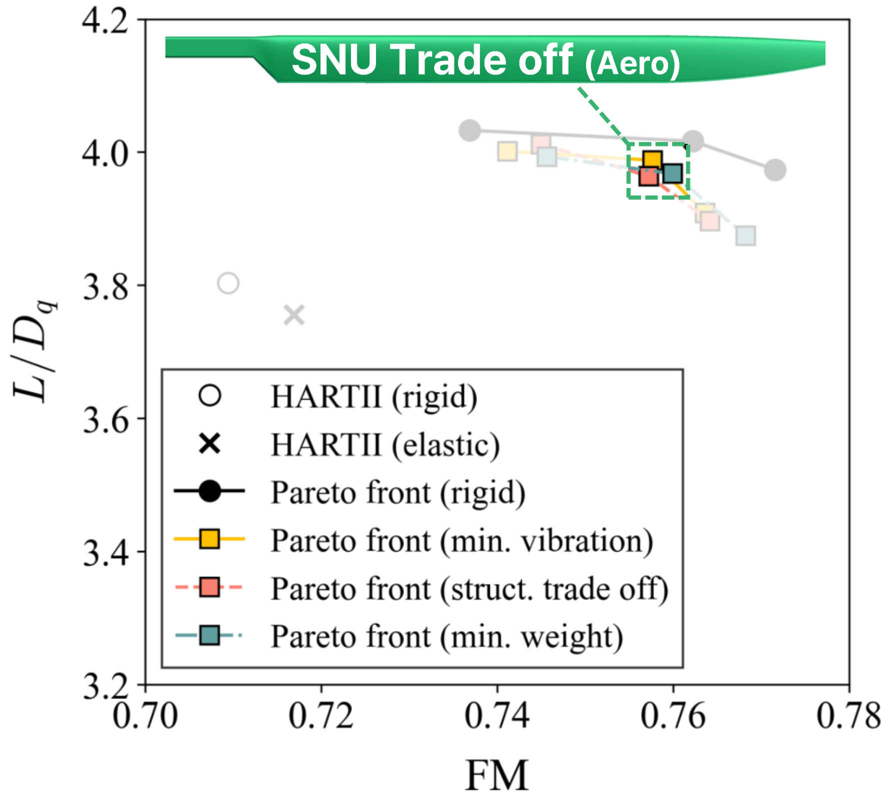

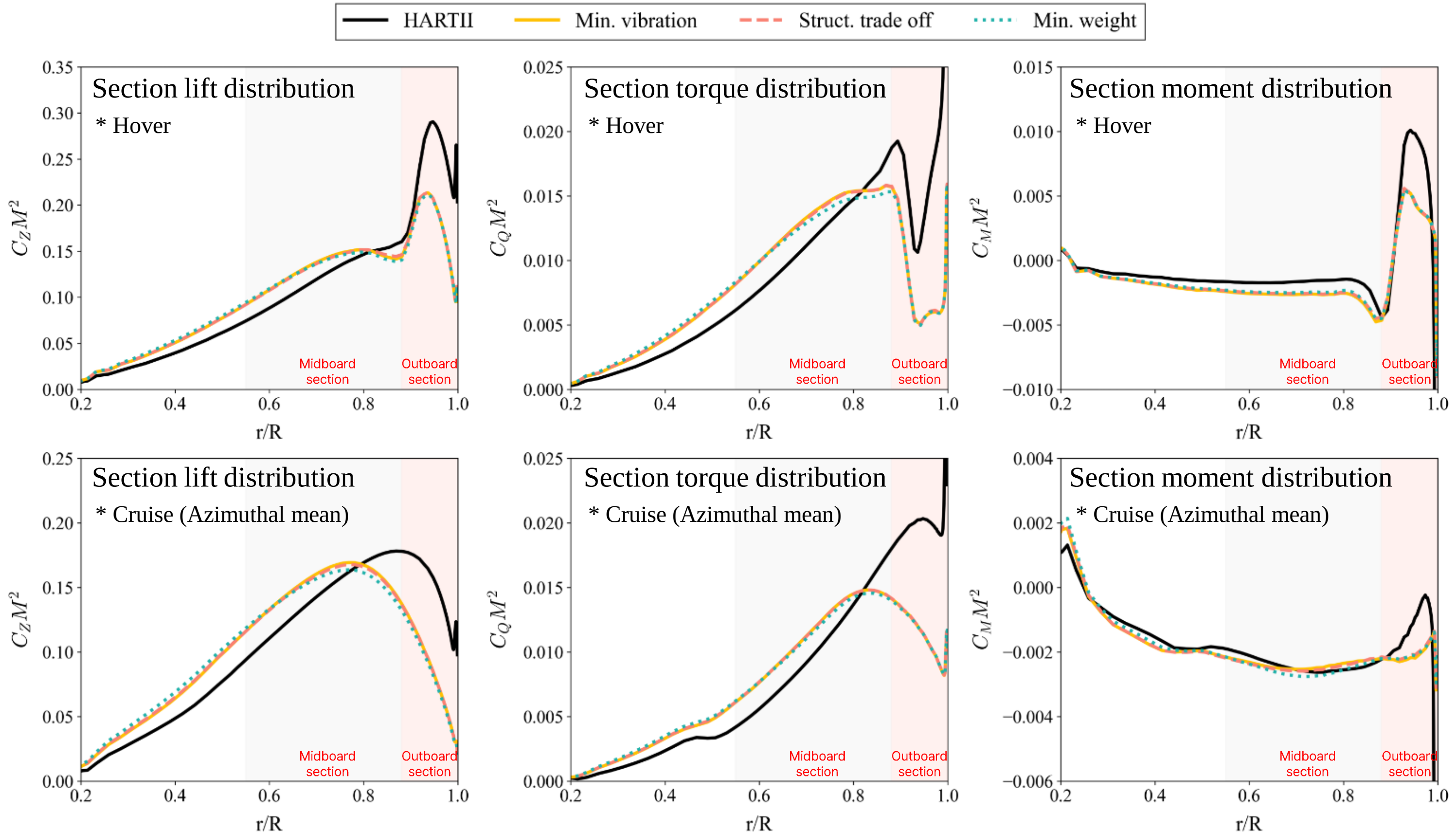

Aeroelastic Implications of Structural Design

- **Flight Condition:** $C_T/\sigma = 0.1$, $M_{tip} = 0.64$ (Hover)
  $\mu = 0.3$, $C_T/\sigma = 0.1$, $C_X/\sigma = 0.00944$ (Cruise)

Aeroelastic Effects of **Different Structural Optimization Objectives** (based on the SNU Trade off blade)

- Three structure designs (Min. vibration / Struct. Trade off / Min. weight) shows **similar aerodynamic loads**
- However, they show **different structural deformations** with different internal structures

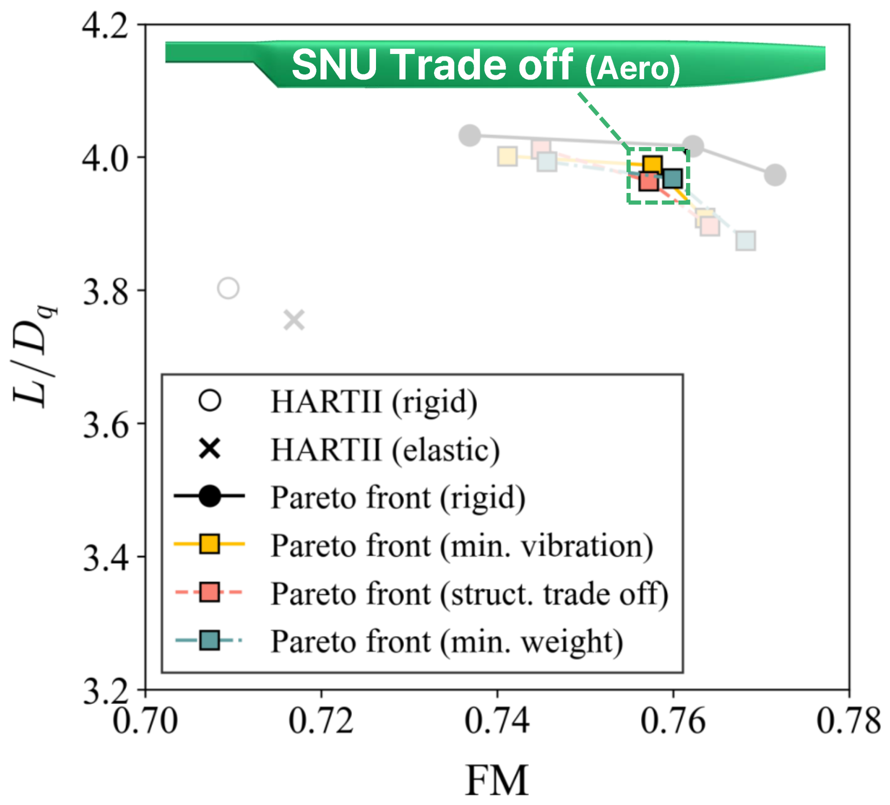

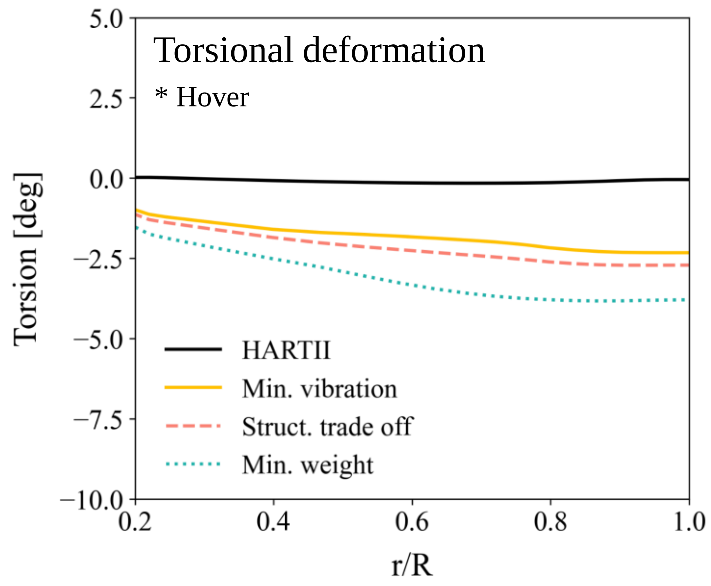

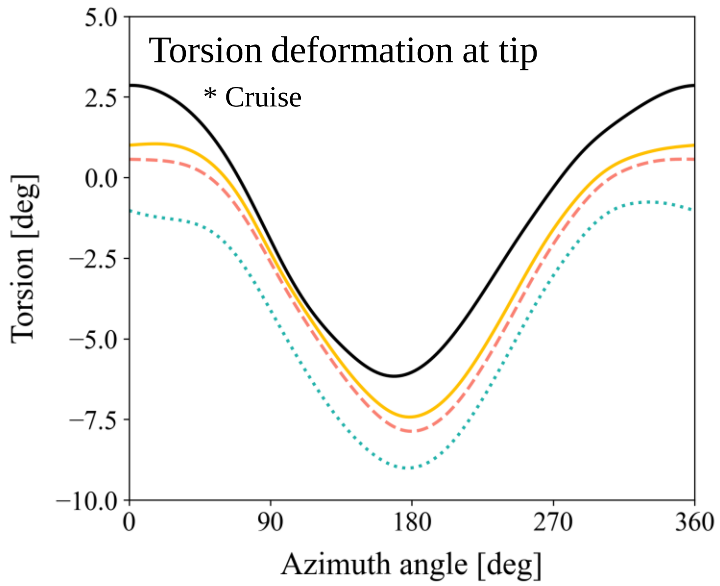

Lighter structural designs reduce torsion stiffness
→ Min. weight blade has largest torsional deformation

Designs focusing on vibration reduction enhance stiffness
→ Min. vibration blade has smallest torsional deformation

Aeroelastic Implications of Structural Design

Comparison Between **Scaling Method** and **Actual Structural Design**

- Optimized blades with min. vibration structural design are selected as representative blades of actual structural design
- Performance difference between scaling method and actual structural design is less than 2%
- Scaling method reasonably approximates aeroelastic effects during aerodynamic design optimization

▶ **Pareto fronts** of scaling method and structural design

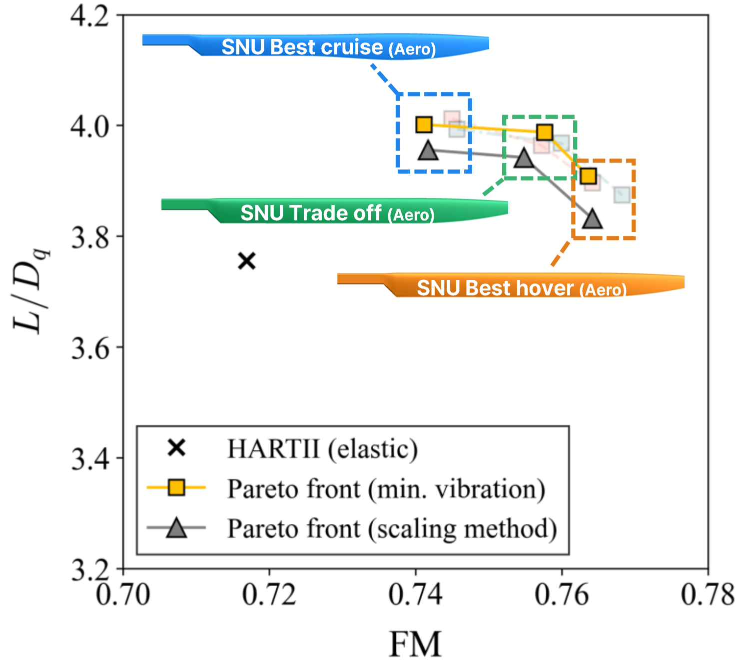

▶ **Performance change** of elastic blades with actual structural design and scaling method vs. rigid blades

	$\Delta FM = (FM_{sc} - FM_{sd})/FM_{sd}$
SNU Best cruise	0.1%
SNU Trade off	-0.4%
SNU Best hover	-0.0%

	$\Delta L/D_q = (L/D_{q_{sc}} - L/D_{q_{sd}})/L/D_{q_{sd}}$
SNU Best cruise	-1.1%
SNU Trade off	-1.2%
SNU Best hover	-1.9%

Nomenclature : (sc : scaling method, sd : structural design)

Aeroelastic Implications of Structural Design

- **Flight Condition:** $C_T/\sigma = 0.1$, $M_{tip} = 0.64$ (Hover)
  $\mu = 0.3$, $C_T/\sigma = 0.1$, $C_X/\sigma = 0.00944$ (Cruise)

Comparison Between **Scaling Method** and **Actual Structural Design**

- Scaling method-based design lacks margin in the **2nd lag mode**
- Actual structural design (Min. vibration) demonstrates sufficient frequency margin in all modal responses

→ **Actual structural design is necessary** to ensure adequate frequency margin

▶ **Pareto fronts** of scaling method and structural design

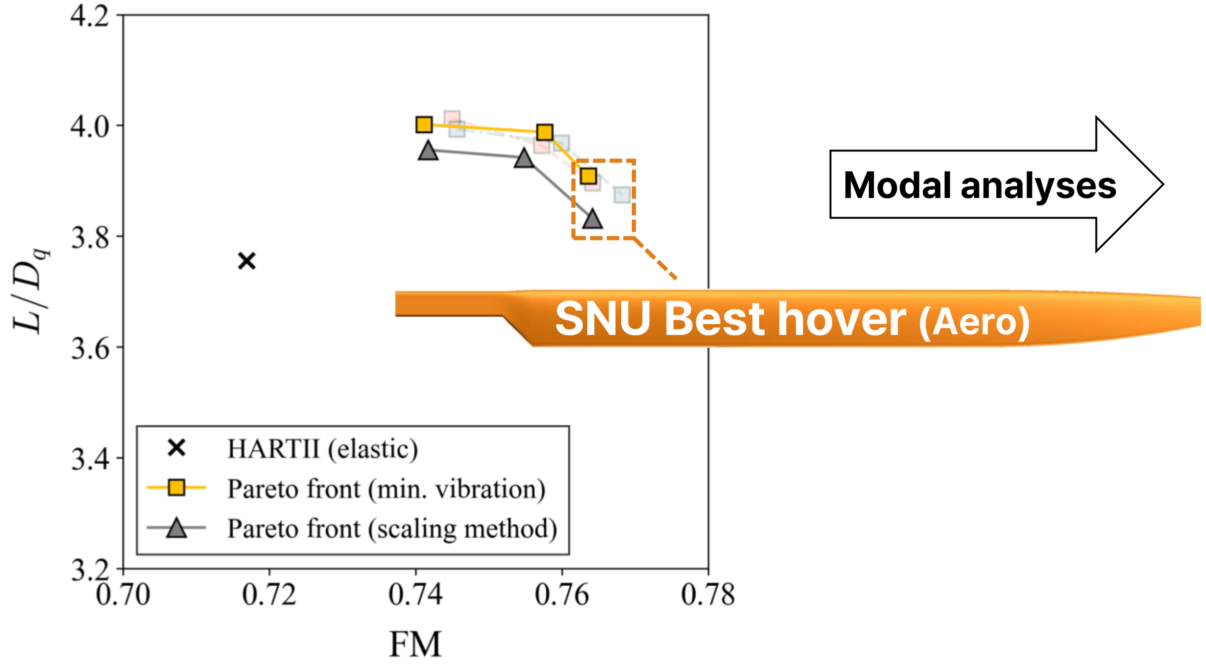

▶ **Frequency diagram** of HART II and SNU Best hover blades with scaling approach and Min. vibration structural design

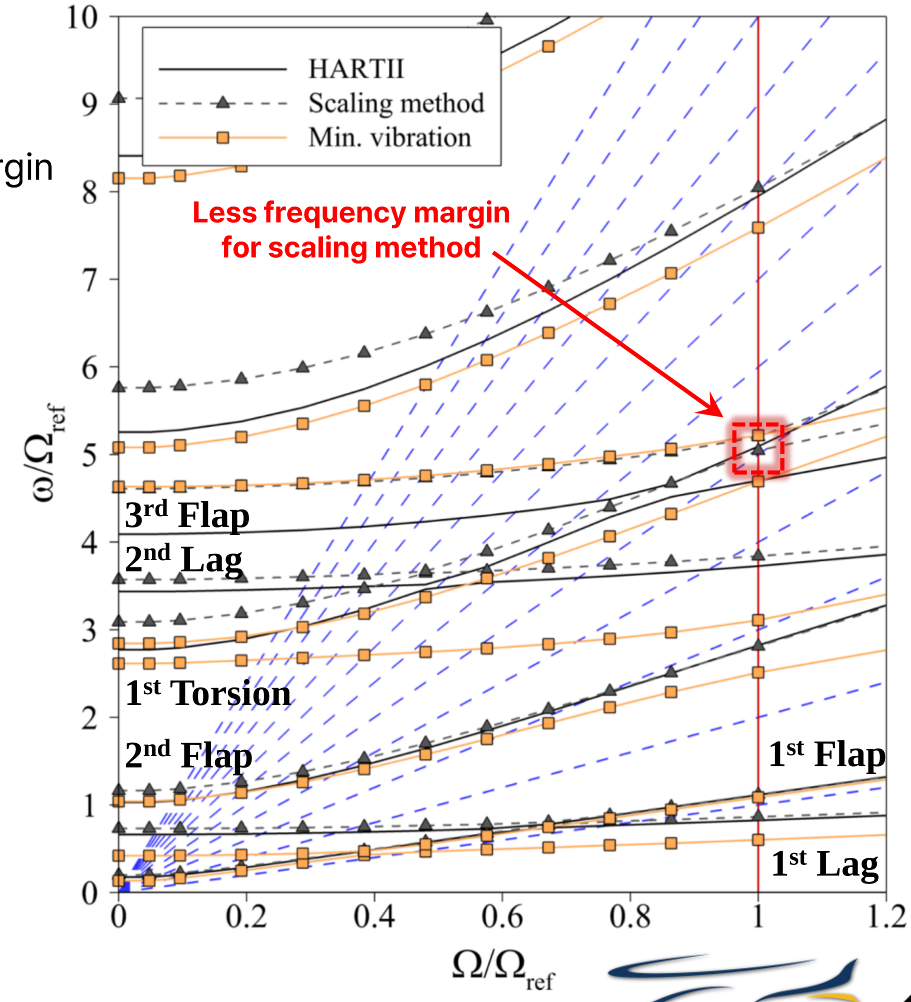

Contents

- Introduction
- Methodology
- Optimization Tasks
- Baseline Results
- **Optimization Results : Comparative Study of Optimized Rotor Blades**
- Conclusion

Comparative Study of Optimized Rotor Blades

- **Flight Condition:** $C_T/\sigma = 0.1$, $M_{tip} = 0.64$ (Hover)
  $\mu = 0.3$, $C_T/\sigma = 0.1$, $C_X/\sigma = 0.00944$ (Cruise)

Comparative Study of Optimized Rotor Blades from SNU and DLR

- Comparison in design hover and cruise condition (based on **SNU Trade off with Min. vibration** and **DLR Balanced with Min. vibration**)

SNU Trade off (with Min. vibration) | **DLR Balanced (with Min. vibration)**

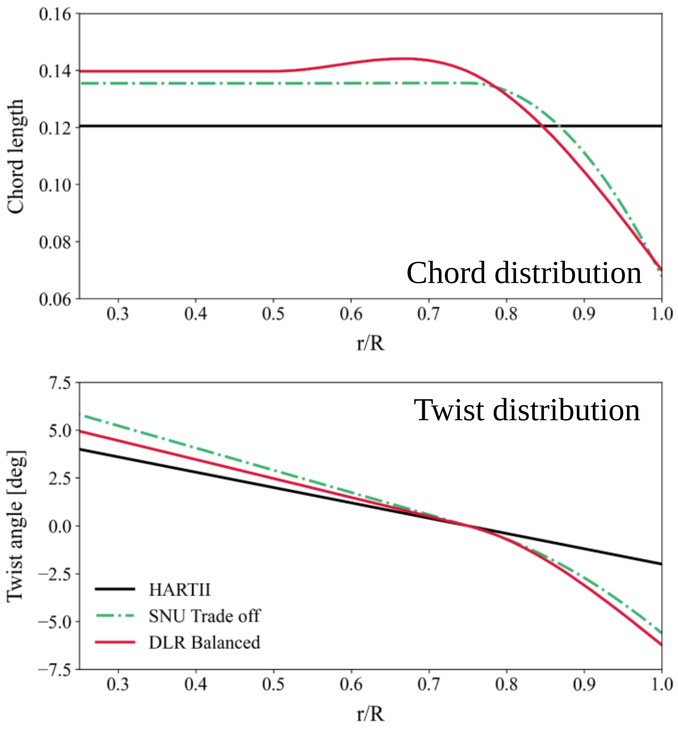

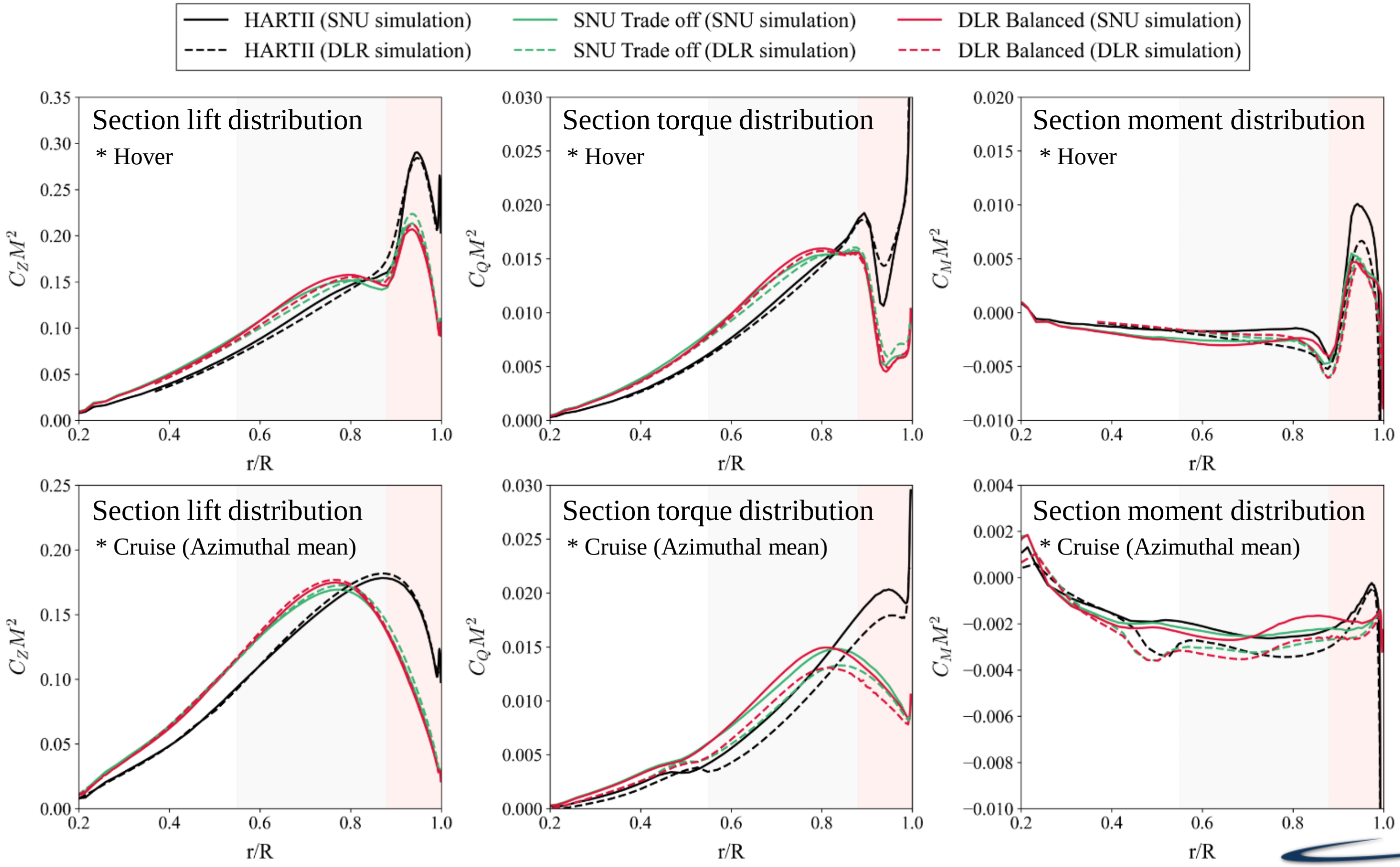

Comparative Study of Optimized Rotor Blades

- **Flight Condition:** $C_T/\sigma = 0.1$, $M_{tip} = 0.64$ (Hover)
  $\mu = 0.3$, $C_T/\sigma = 0.1$, $C_X/\sigma = 0.00944$ (Cruise)

Comparative Study of Optimized Rotor Blades from SNU and DLR

- Comparison in design hover and cruise condition (based on **SNU Trade off with Min. vibration** and **DLR Balanced with Min. vibration**)

Hover : Sectional performance of the optimized blades shows high **consistency** between the SNU and DLR simulations

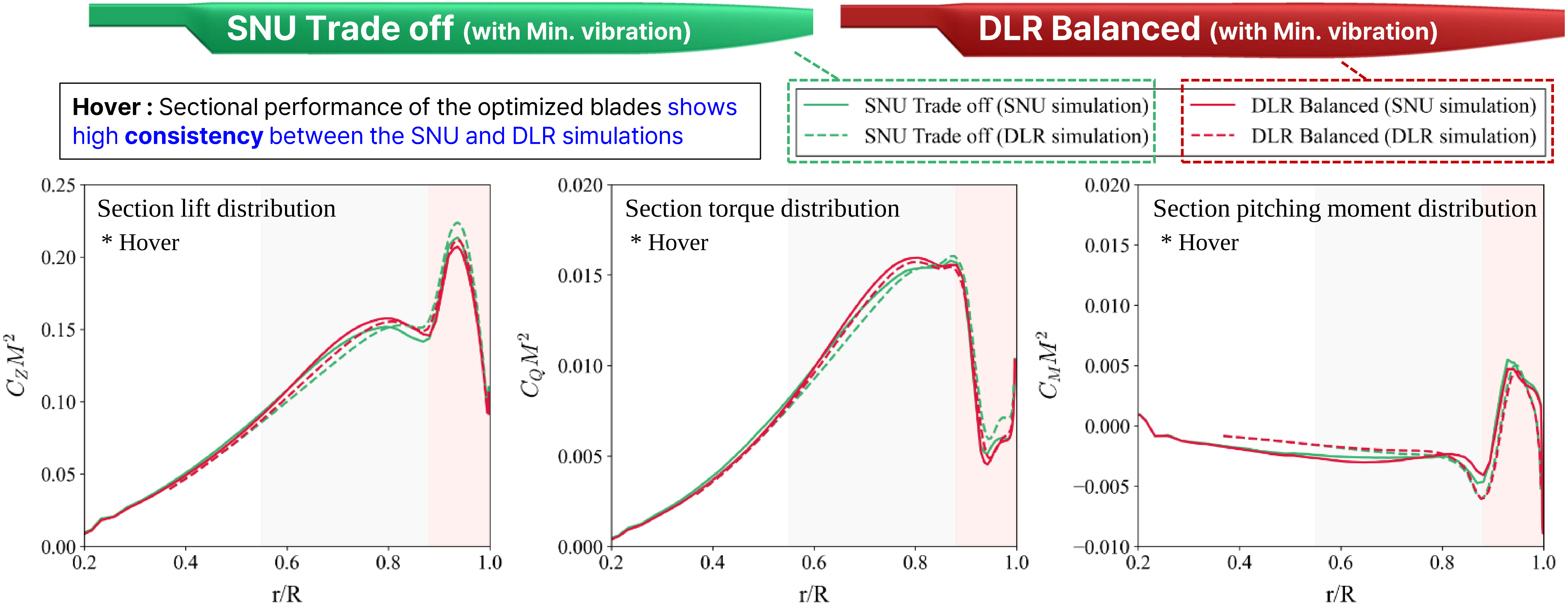

Comparative Study of Optimized Rotor Blades

- **Flight Condition:** $C_T/\sigma = 0.1$, $M_{tip} = 0.64$ (Hover)
  $\mu = 0.3$, $C_T/\sigma = 0.1$, $C_X/\sigma = 0.00944$ (Cruise)

Comparative Study of Optimized Rotor Blades from SNU and DLR

- Comparison in design hover and cruise condition (based on **SNU Trade off with Min. vibration** and **DLR Balanced with Min. vibration**)

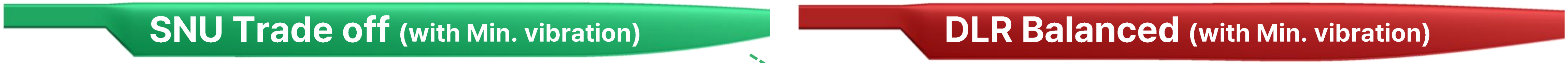

Cruise : Torque computed by the SNU simulation are slightly **higher** due to fully turbulent assumption in the SNU's CFD approach

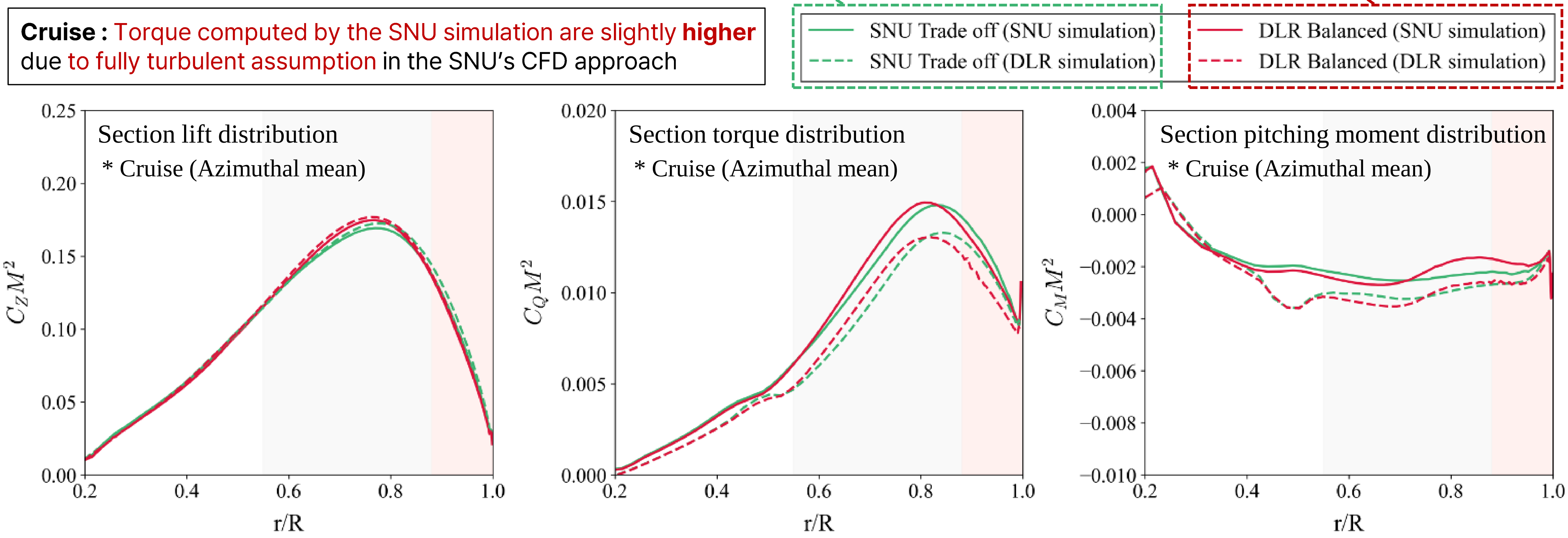

Comparative Study of Optimized Rotor Blades

- **Flight Condition:** $C_T/\sigma = 0.1$, $M_{tip} = 0.64$ (Hover)
  $\mu = 0.3$, $C_T/\sigma = 0.1$, $C_X/\sigma = 0.00944$ (Cruise)

■ **Comparative Study** of Optimized Rotor Blades **from SNU and DLR**

- **Comparison in off-design conditions → Both optimized blade are highly similar in both performance and shape**

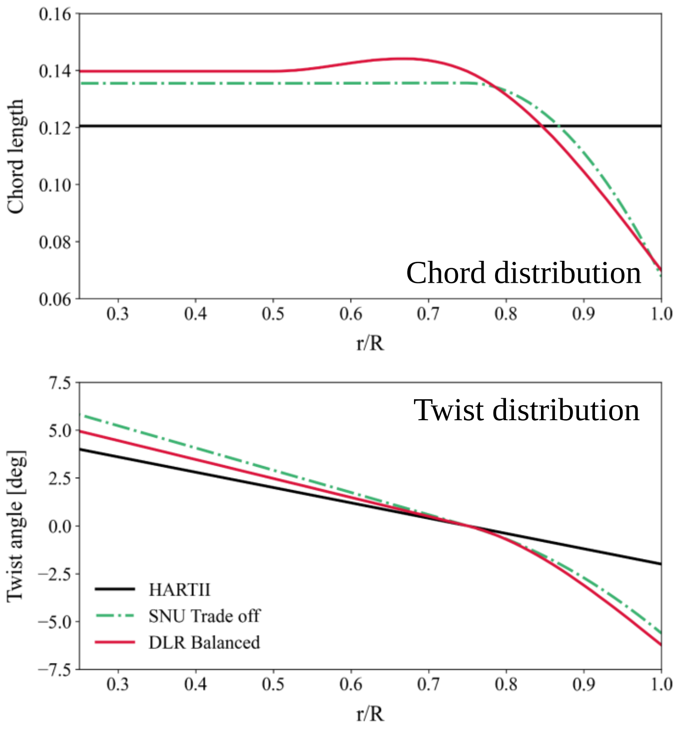

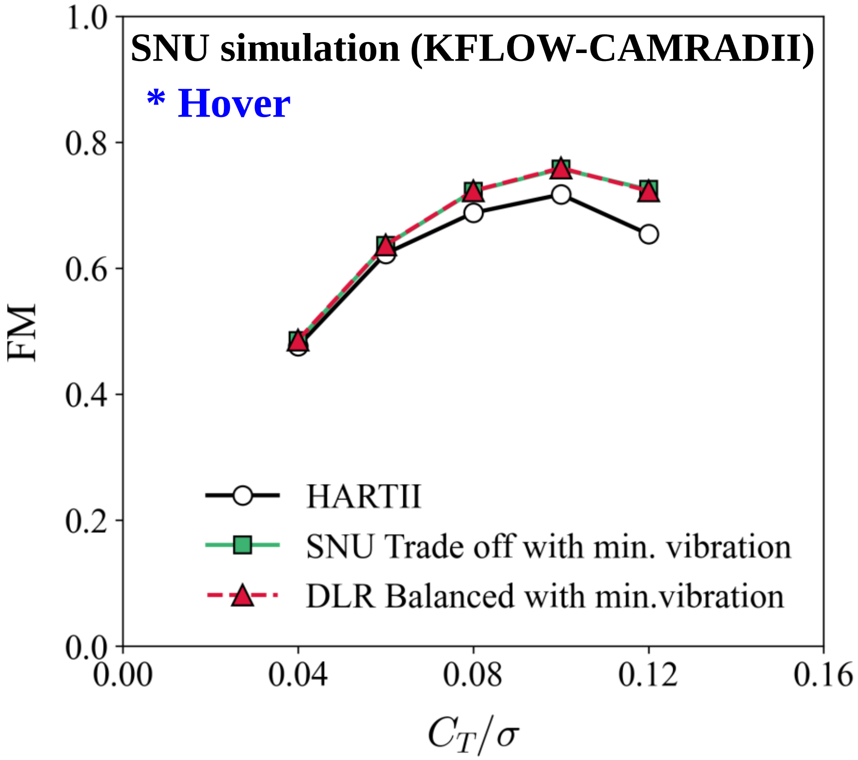

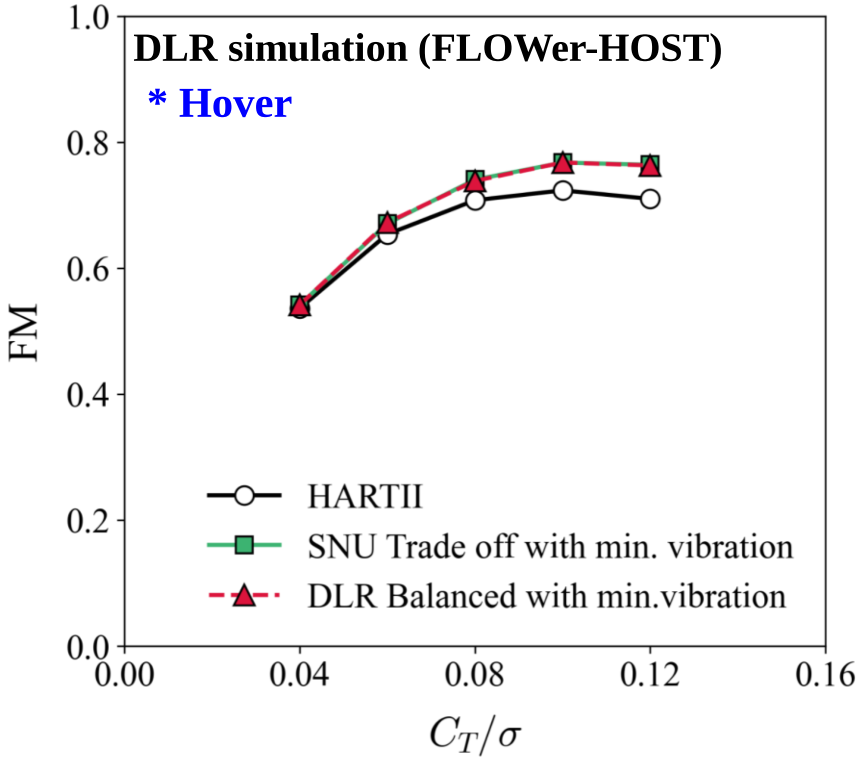

Comparative Study of Optimized Rotor Blades

- **Flight Condition:** $C_T/\sigma = 0.1$, $M_{tip} = 0.64$ (Hover)
  $\mu = 0.3$, $C_T/\sigma = 0.1$, $C_X/\sigma = 0.00944$ (Cruise)

Comparative Study of Optimized Rotor Blades **from SNU and DLR**

- **Comparison in off-design conditions → Both optimized blade are highly similar in both performance and shape**

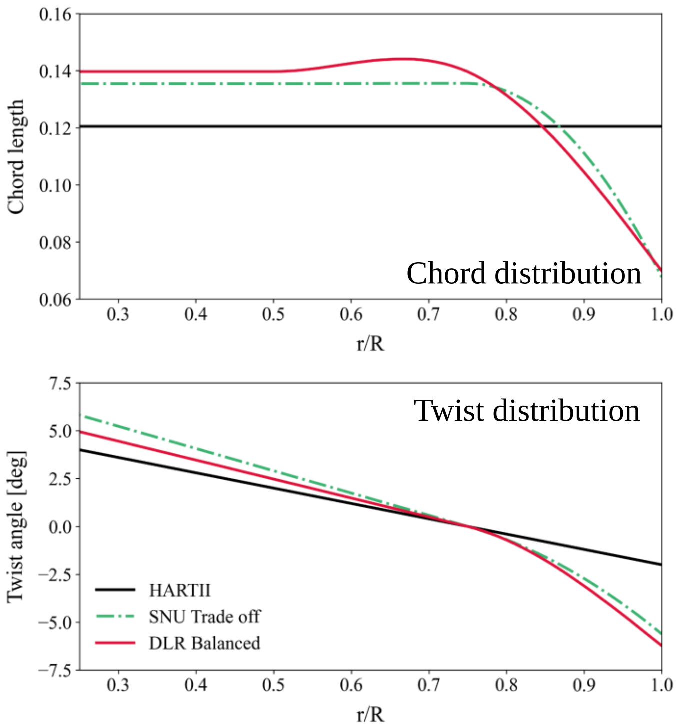

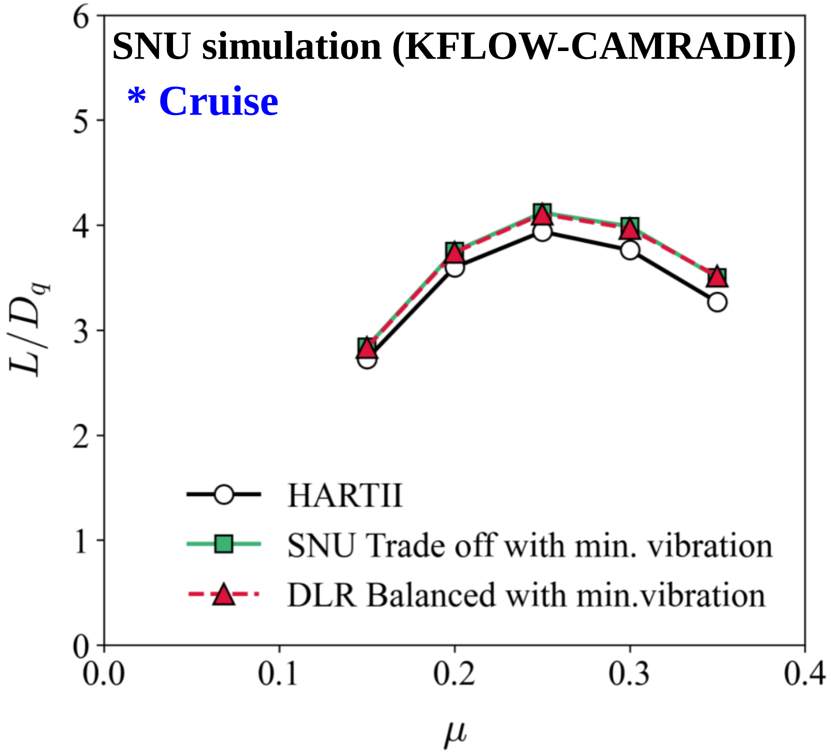

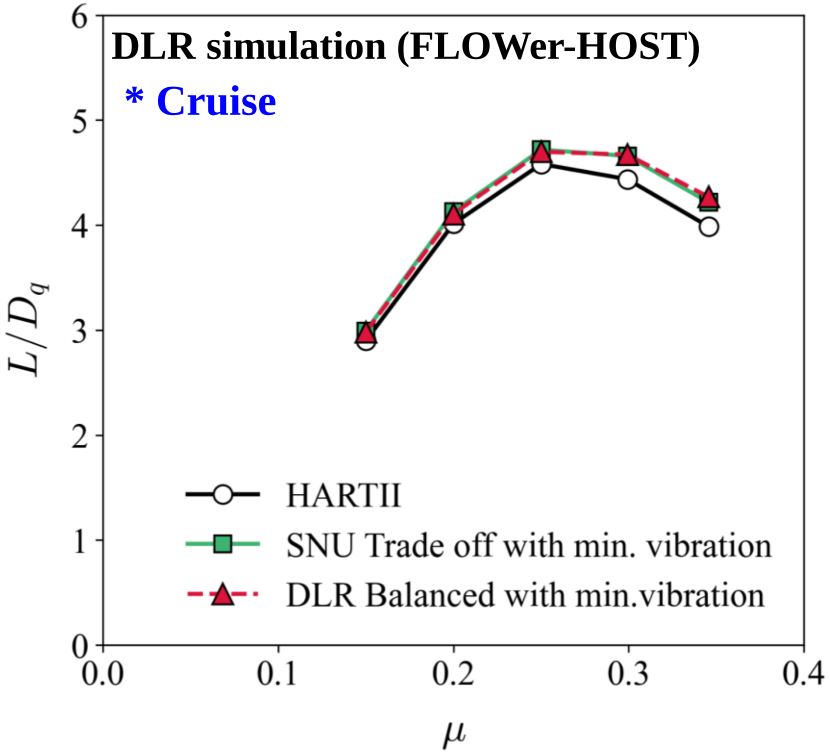

Contents

- Introduction
- Methodology
- Optimization Tasks
- Baseline Results
- Optimization Results
- **Conclusion**

CONCLUSION

SNU Trade off blade with min. vibration structural design

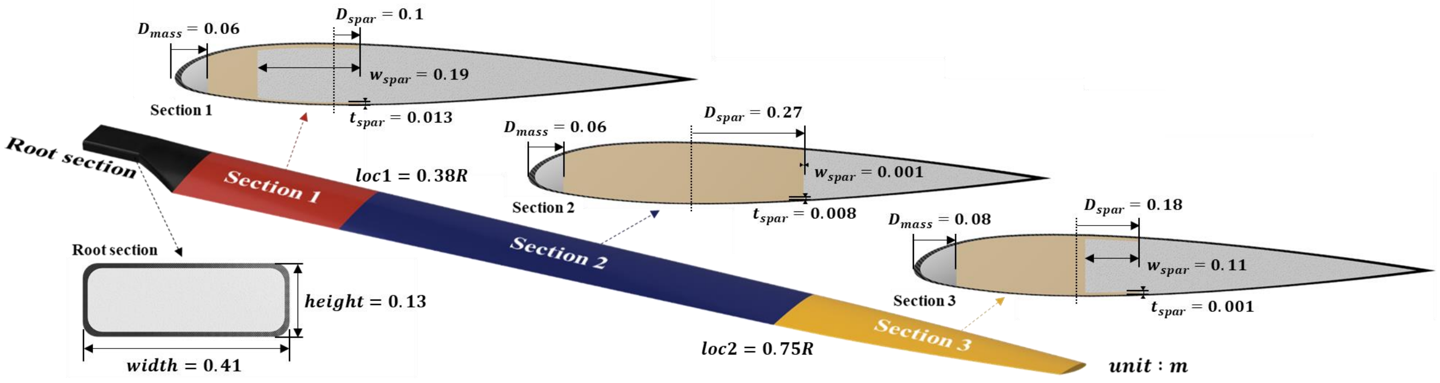

■ Summary

- A high-fidelity simulation-based framework has been developed for rotor blade design, combining **aerodynamic and structural optimization**

■ Key Results

- **Performance Improvements**
  - ✓ Up to **6.5% FM improvement** (Best Hover blade) and **6.6% L/D_q improvement** (Best Cruise blade) over HART II **with actual internal structure :** tapered and twisted tip designs reduce the torque at tip and improve aerodynamic efficiency
- **Effect of Structural Design**
  - ✓ **Aerodynamic performance difference from different structural designs is less than 2%**
    - **Structural design is highly constraint-driven, requiring satisfaction of numerous constraints → design space becomes narrow**
  - ✓ **Only full structural design optimization guarantees structural dynamic feasibility** (e.g., frequency margins)
- **Cross-Institutional Validation**
  - ✓ Despite differences in solvers and methods, **SNU and DLR obtain similar blade shapes and aerodynamic performance**
    - With aligned simulation setups and parameterizations, **different solvers yield similar performance and blade shapes**

Thank You

Seongjoong Park
M.S. Candidate
eric2237@snu.ac.kr

This research was supported by Korean Institute for Advancement of Technology(KIAT) grant funded by the Korea Government(MOTIE) (RS-2024-00436124, Human Resource Development Program for Industrial Innovation(Global))

The authors thank Professor Soo Hyung Park for providing the KFLOW source code and also thank Professor Sung Nam Jung for providing the Ksec2d-AE for the current study

APPENDIX

Aerodynamic Design

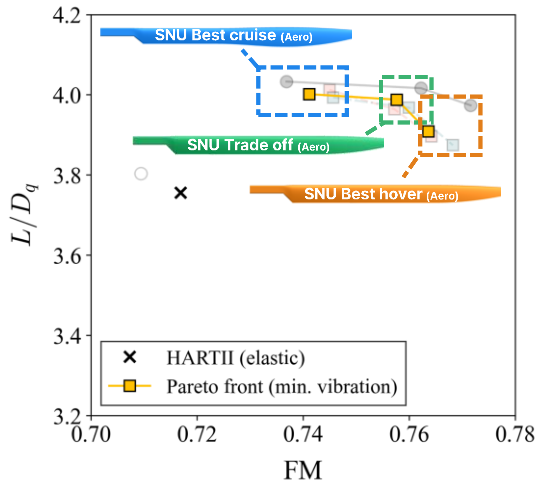

- **Hover** performance analysis (Min. vibration designs)
  - Performance gain due to **reduced inflow and induced drag**
    - ✓ **Weaker tip vortices** decreases inflow velocity and induced drag
    - ✓ Increased tip twist and reduced tip chord length weakens the tip vortices

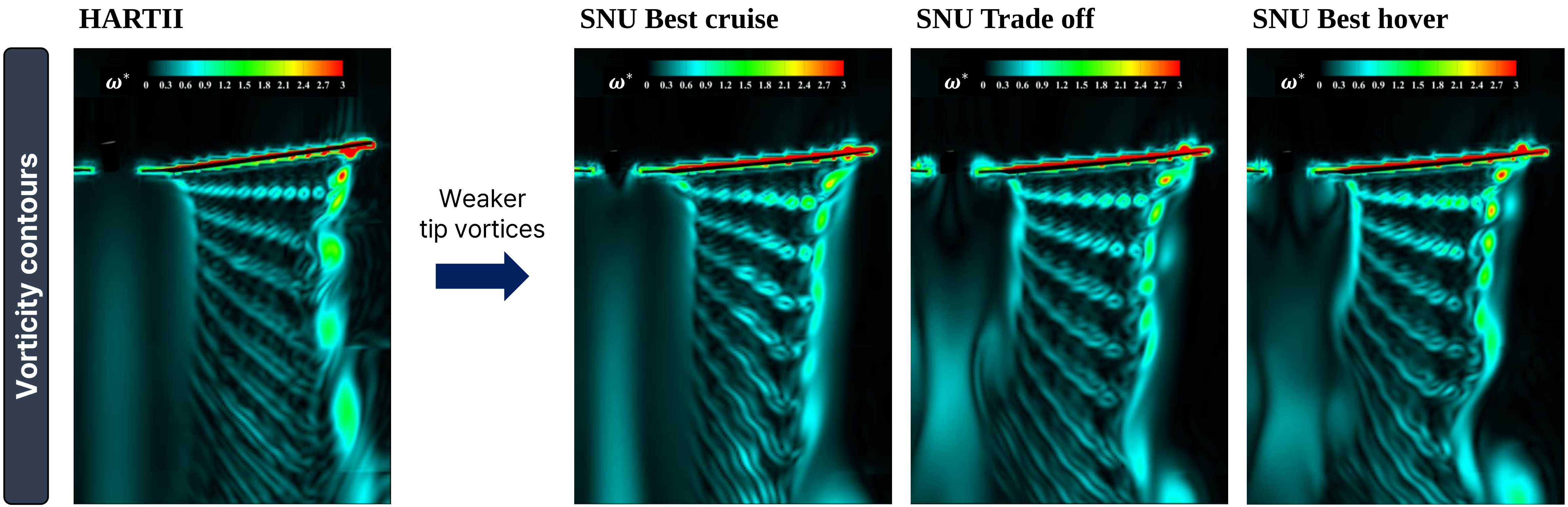

ω^*: non-dimensional vorticity magnitude

Aerodynamic Design

- **Cruise** performance analysis (Min. vibration designs)
  - Performance gain due to **off-loaded outboard**
    - ✓ Reduced tip AOA due to increased tip twist
    - ✓ Excessive twist degrades performance

→ Less airload in outboard leads to performance enhancement

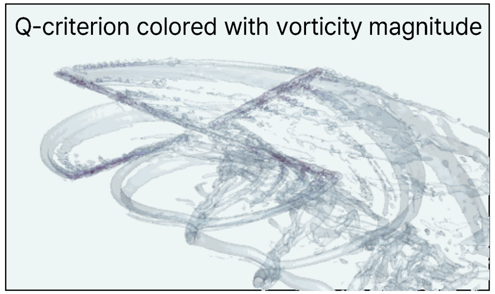

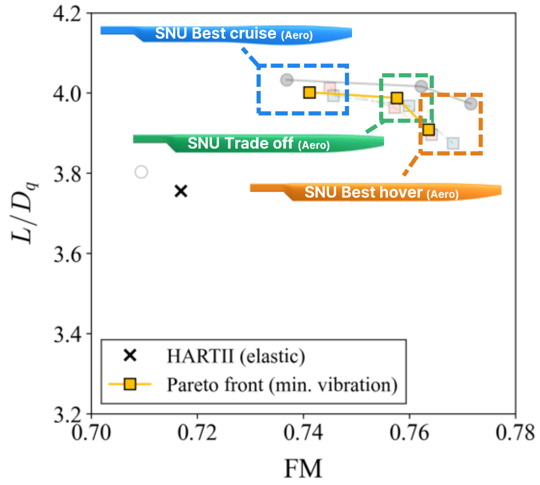

SNU Best cruise (L/D_q : 4.001 ↑6.9%)

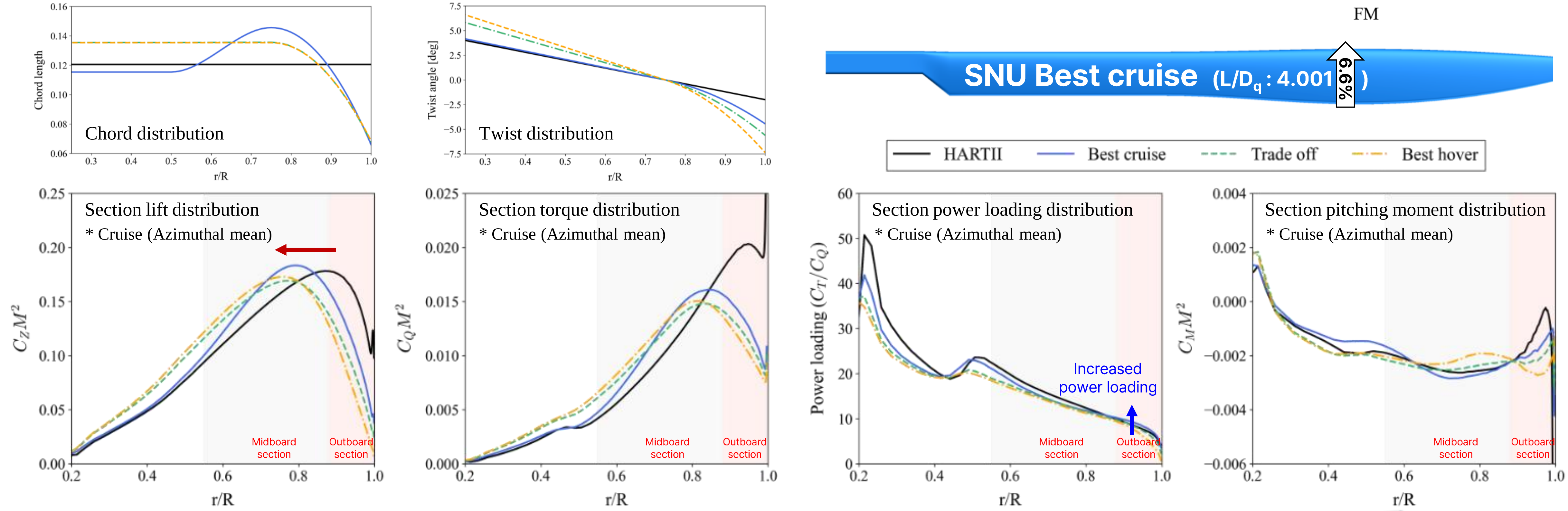

STRUCTURAL DESIGN

- Objectives and **Constraints** of Optimum Designs from Structural Design

	Constraint value	SNU Best hover		SNU Trade off		SNU Best cruise		DLR Balanced	
		MV	MW	MV	MW	MV	MW	MV	MW
Blade Mass, kg	-	3.42	2.68	3.20	2.74	3.17	2.92	3.39	2.98
VI	-	0.008	0.012	0.009	0.013	0.011	0.013	0.011	0.014
Autorotation Index	**0.00613**	**0.00613**	**0.00613**	**0.00613**	**0.00613**	**0.00613**	**0.00613**	**0.00613**	**0.00613**
Center of Gravity (distance from quarter chord line, %)	0.0500	0.0457	0.0341	0.0308	0.0445	0.0231	0.0354	0.0472	0.0384
Tip flap deformation, w/R	**0.0450**	**0.0448**	**0.0449**	**0.0443**	**0.0450**	**0.0447**	**0.0448**	**0.0450**	**0.0449**
Lag 1st Frequency Margin, /rev	**0.1000**	0.0567	**0.0961**	0.0803	0.0969	0.0807	0.0786	0.0224	0.0334
Flap 2nd Frequency Margin, /rev	0.4000	0.3266	0.0102	**0.3872**	0.1678	0.2700	0.2296	0.3150	0.1710
Torsion 1st Frequency Margin, /rev	**0.4000**	0.2319	**0.3929**	0.2878	0.3794	0.3454	0.3383	**0.3960**	0.3550
Lag 2nd Frequency Margin, /rev	**0.4000**	0.3125	0.1956	0.1761	0.3714	0.3319	0.3612	**0.3880**	0.3530
Flap 3rd Frequency Margin, /rev	**0.4000**	0.3321	0.2693	0.2075	0.3131	0.1312	0.1628	0.3380	**0.3940**

Structural Design

- Structural Design Results

			BH_MW	BH_MV	TO_MW	TO_MV	BC_MW	BC_MV	DLR_MW	DLR_MV	up	lb	BH_MW	BH_MV	TO_MW	TO_MV	BC_MW	BC_MV	DLR_MW	DLR_MV
root section		DV00	0.99995	0.87229	0.9456	0.92763	0.83932	0.83435		0.889										
		DV01	0.31898	0.225206	0.56312	0.44906	0.58244	0.16171		0.186										
	height	DV02	0.15869	0.149835	0.01526	0.00904	0.50727	0.52005		0.0181	0.29	0.13	0.15539	0.15397	0.13244	**0.13145**	**0.21116**	**0.21321**	0.13	**0.1329**
	width	DV03	0.19807	0.097272	0.1893	0.14336	0.08265	0.14015		0.687	0.62	0.37	0.41952	0.39432	0.41732	**0.40584**	0.39066	0.40504	0.37	**0.54175**
Airfoil section1		DV04	0.75854	0.046221	0.50855	0.28908	0.47094	0.55177		0.289										
	t_spar	DV05	0.62891	0.726411	0.15473	0.83793	0.48844	0.66459		0.218	0.015	0.001	0.0098	0.01117	**0.00317**	**0.01273**	0.00784	0.0103	0.001	**0.00405**
	D_spar	DV06	0.02255	0.081383	0.06728	0.01664	0.14573	0.01151		0.00027	0.3	0.1	0.10451	0.11628	0.11346	**0.10333**	0.12915	0.1023	0.1	**0.10005**
	w_spar	DV07	0.70433	0.926112	0.90395	0.97744	0.938	0.93371		0.993	0.2	0	0.14087	0.18522	0.18079	**0.19549**	0.1876	0.18674	0	**0.1986**
	D_mass	DV08	0.16653	0.170629	0.24738	0.2572	0.49216	0.49735		0.00688	0.1	0.05	0.05833	0.05853	0.06237	**0.06286**	0.07461	0.07487	0.05	**0.05034**
loc1		DV09	0.46053	0.328534	0.4806	0.42272	0.41445	0.42005		0.355	0.5	0.3	0.39211	0.36571	0.39612	**0.38454**	0.38289	0.38401	0.3	**0.371**
Airfoil section2		DV10	0.36839	0.765513	0.04818	0.09336	0.76002	0.31098		0.625										
	t_spar	DV11	0.01567	0.987862	0.55868	0.51402	0.62746	0.57143		0.998	0.015	0.001	0.00122	0.01483	0.00882	**0.0082**	0.00978	0.009	0.001	**0.01497**
	D_spar	DV12	0.1325	0.938104	0.00218	0.88835	0.7482	0.98433		0.965	0.3	0.1	0.1265	0.28762	0.10044	**0.27767**	0.24964	0.29687	0.1	**0.293**
	w_spar	DV13	0.94953	0.042013	0.37474	0.00545	0.94305	0.07332		0.977	0.2	0	0.18991	0.0084	0.07495	**0.00109**	0.18861	0.01466	0	**0.1954**
	D_mass	DV14	0.50957	0.305628	0.4279	0.34321	0.4817	0.449		0.519	0.1	0.05	0.07548	0.06528	0.07139	**0.06716**	0.07408	0.07245	0.05	**0.07595**
loc2		DV15	0.79821	0.798237	0.77795	0.74533	0.77086	0.75807		0.685	0.8	0.6	0.75964	0.75965	0.75559	**0.74907**	0.75417	0.75161	0.6	**0.737**
Airfoil section3		DV16	0.00964	0.010062	0.0133	0.02352	0.03875	0.0499		0.0596										
	t_spar	DV17	0.02341	0.02151	0.0371	0.03505	0.9536	0.98959		0.0472	0.015	0.001	0.00133	0.0013	0.00152	**0.00149**	0.01435	0.01485	0.001	**0.00166**
	D_spar	DV18	0.88106	0.114083	0.7801	0.41639	0.06393	0.05199		0.248	0.3	0.1	0.27621	0.12282	0.25602	**0.18328**	0.11279	0.1104	0.1	**0.1496**
	w_spar	DV19	0.78281	0.737987	0.50543	0.52985	0.54678	0.76552		0.293	0.2	0	0.15656	0.1476	0.10109	**0.10597**	0.10936	0.1531	0	**0.0586**
	D_mass	DV20	0.84218	0.804152	0.64642	0.65689	0.92368	0.82111		0.909	0.1	0.05	0.09211	0.09021	0.08232	**0.08284**	0.09618	0.09106	0.05	**0.09545**

Aeroelastic Implications of Structural Design

- **Flight Condition:** $C_T/\sigma = 0.1$, $M_{tip} = 0.64$ (Hover)
  $\mu = 0.3$, $C_T/\sigma = 0.1$, $C_X/\sigma = 0.00944$ (Cruise)

Aeroelastic Effects of **Different Structural Optimization Objectives** (based on the SNU Trade off blade)

- Three structure designs (Min. vibration / Struct. Trade off / Min. weight) shows **similar aerodynamic loads**
- However, they show **different structural deformations** with different internal structures

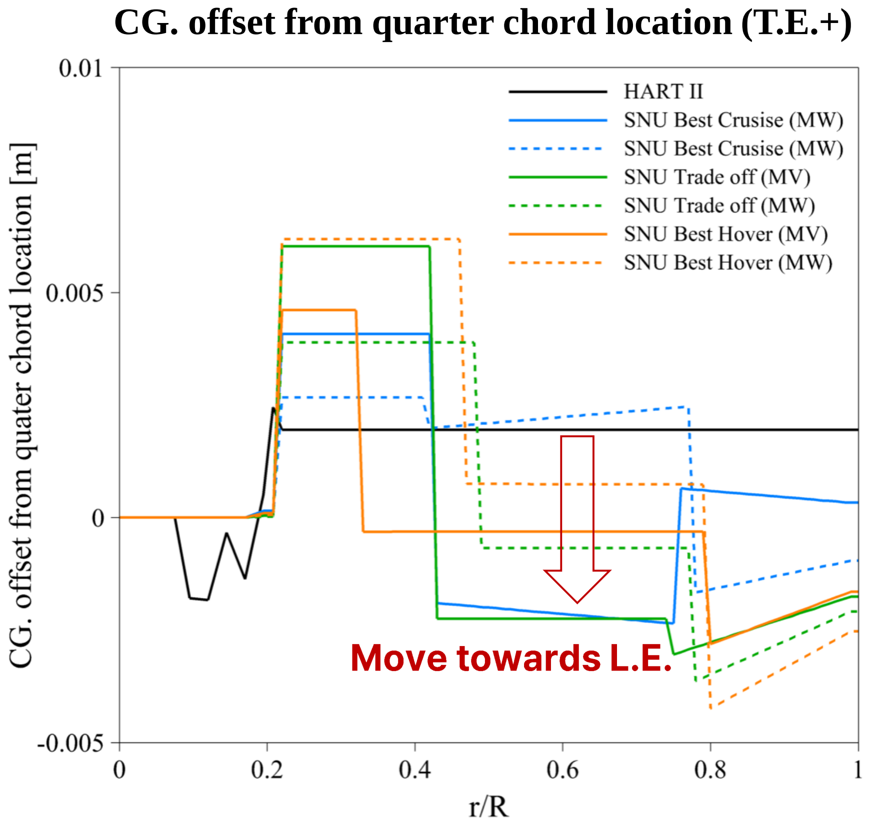

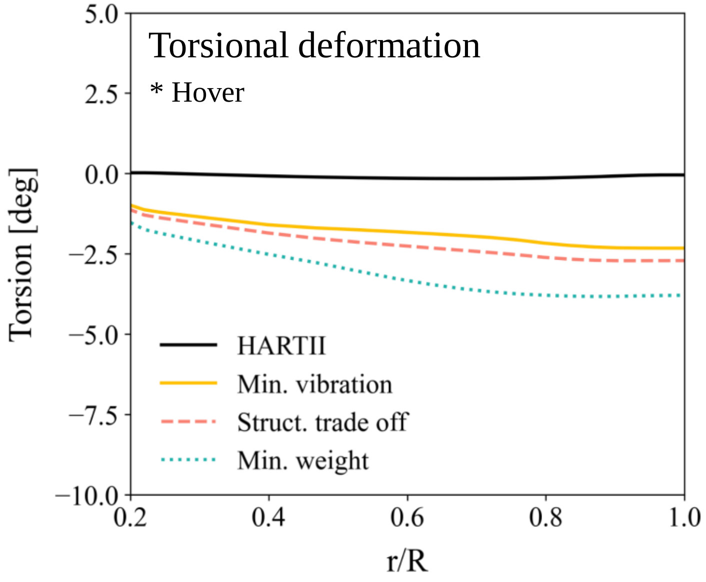

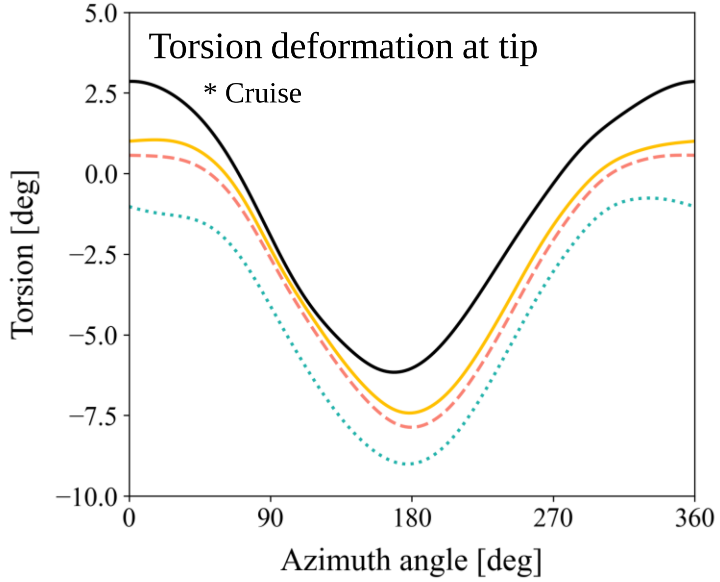

Forward shift of the center of gravity
→ Torsional deformations increase compared to the HART II

STRUCTURAL DESIGN

[1] Lee, D., Multi-disciplinary Design Optimization of Rotor Blades using Data-driven Aero-Structure Performance Modeling, Ph.D. thesis, Seoul National University, 2024

- ANOVA results from previous research (Dawoon Lee's Ph.D thesis[1])

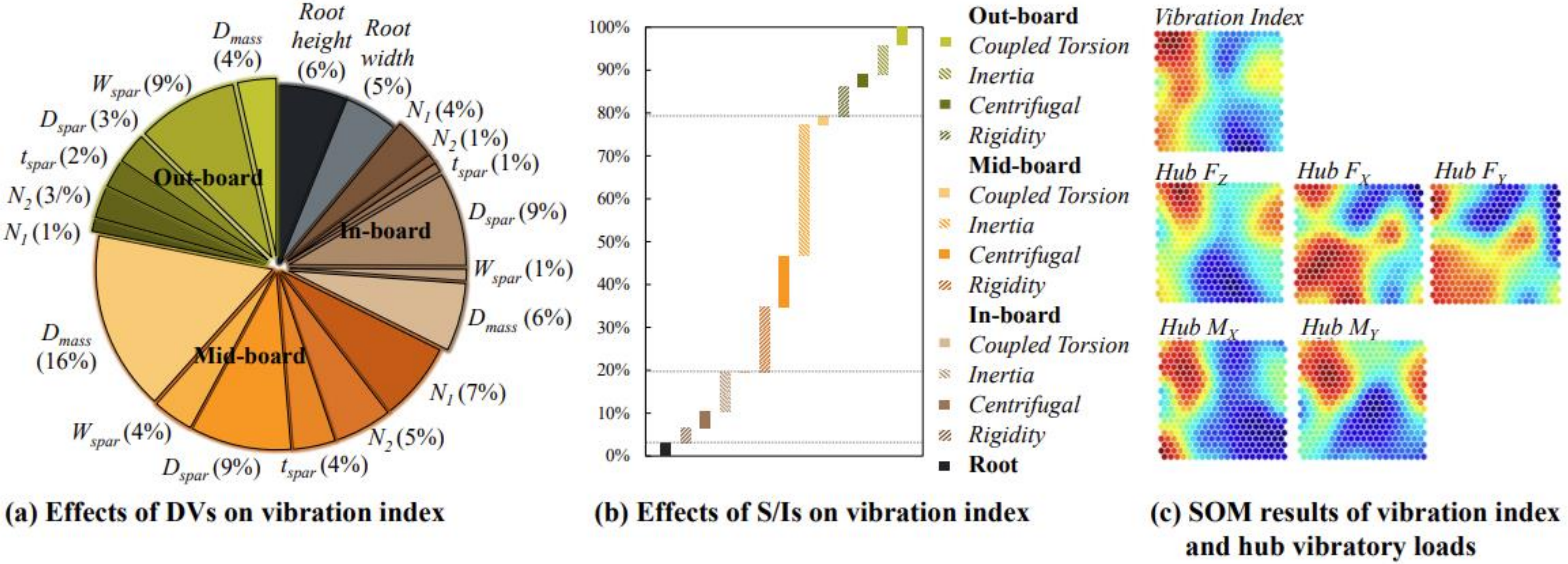

Fig. 2.13. Effects on vibration index and SOM results of hub vibratory loads

METHODOLOGY

Simulations Setups for Blade Outer Shape Optimization

- Low-fidelity solver : CAMRAD II Inflow Model
- Validation results of Low-fidelity solver (CAMRAD II)

Solver details of Low-Fidelity Solver

Solver Details	SNU AVDL
Solver	CAMRAD II
C81 Table	From 2D URANS solver - O-grid Type - 27.8K cells - 5th order eMLP with AUSMPW+ - Steady
Reynolds Correction	Both lift and drag (w/ exp=0.2)
Spanwise panels	26
Rotor motion	Rigid

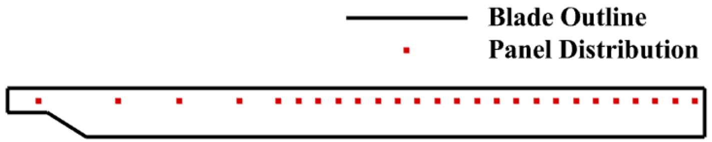

Hover Validation

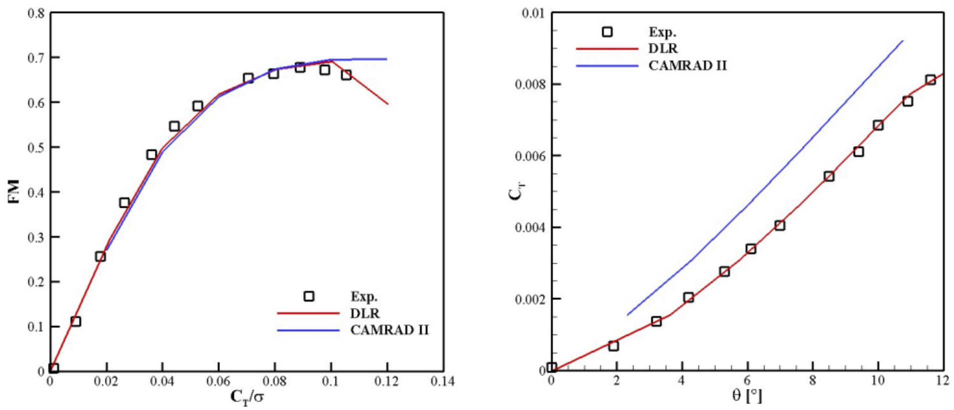

Cruise Validation

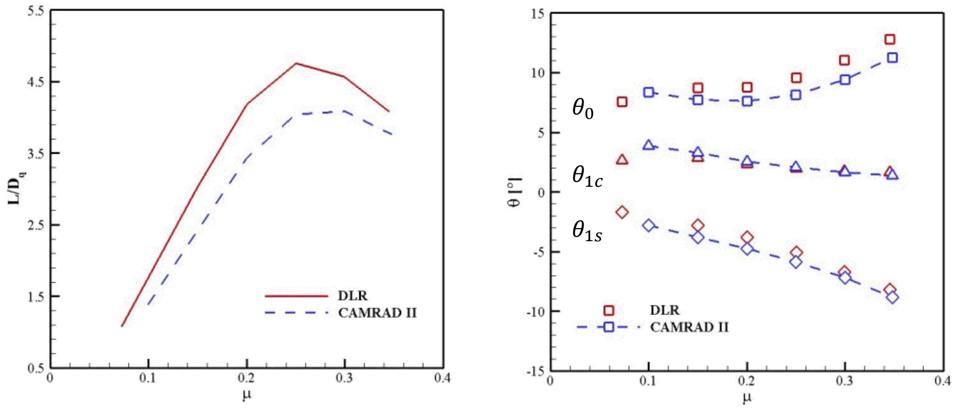

METHODOLOGY

[1] Smith, M. J., Lim, J. W., van der Wall, B. G., Baeder, J. D., Biedron, R. T., Boyd, D. D., Jayaraman, B., Jung, S. N., and Min, B.-Y., "The HARTII International Workshop: An Assessment of the State of the Art in CFD/CSD Prediction," CEAS Aeronautical Journal, Vol. 4, No. 4, 2013, pp. 345–372.

■ CFD/CSD loose coupling method

Validation result (KFLOW-CII) - HART II Experiment Case[1]

	Experiment [1]	FLOWer-HOST	KFLOW-CII	Absolute error
θ_0 [deg]	3.80	3.61	3.42	0.42
θ_{1c} [deg]	1.92	1.58	1.48	0.34
θ_{1s} [deg]	-1.34	-0.66	--0.94	0.40